Supplementary

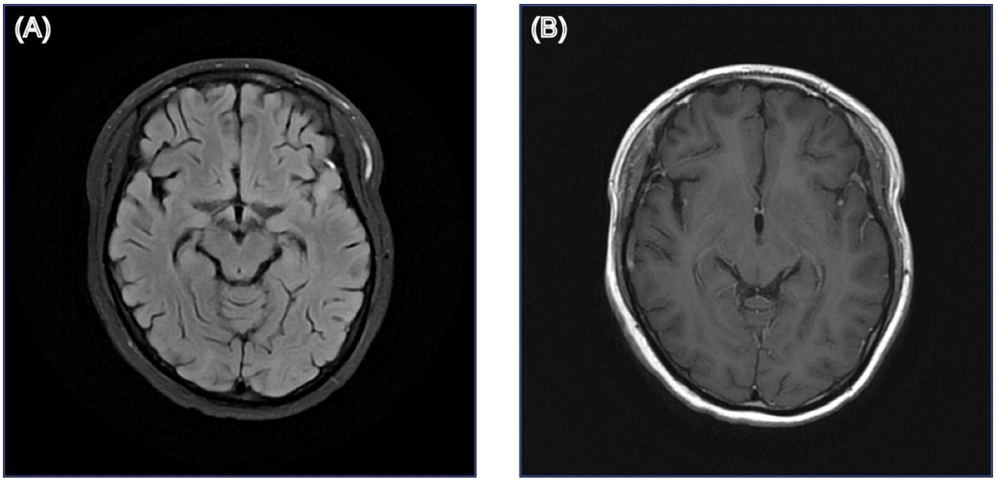

Figure S1 Structural brain MRI images of patient 01. (A) T2-weighted fluid-attenuated inversion recovery (T2-FLAIR) image; (B) Gadolinium-enhanced T1-weighted (Gd-T1w) image.

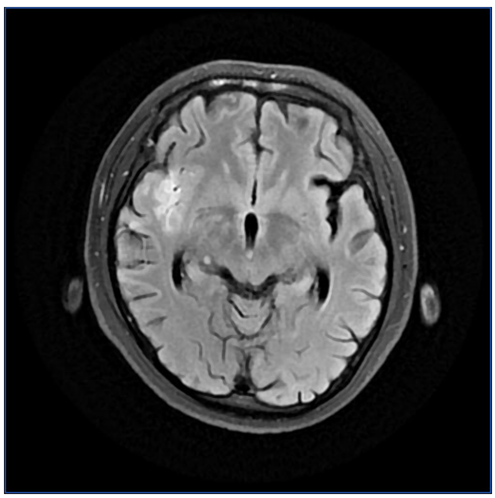

Figure S2 T2-weighted fluid-attenuated inversion recovery (T2-FLAIR) image of patient 02.

https://dx.doi.org/10.21037/qims-22-17

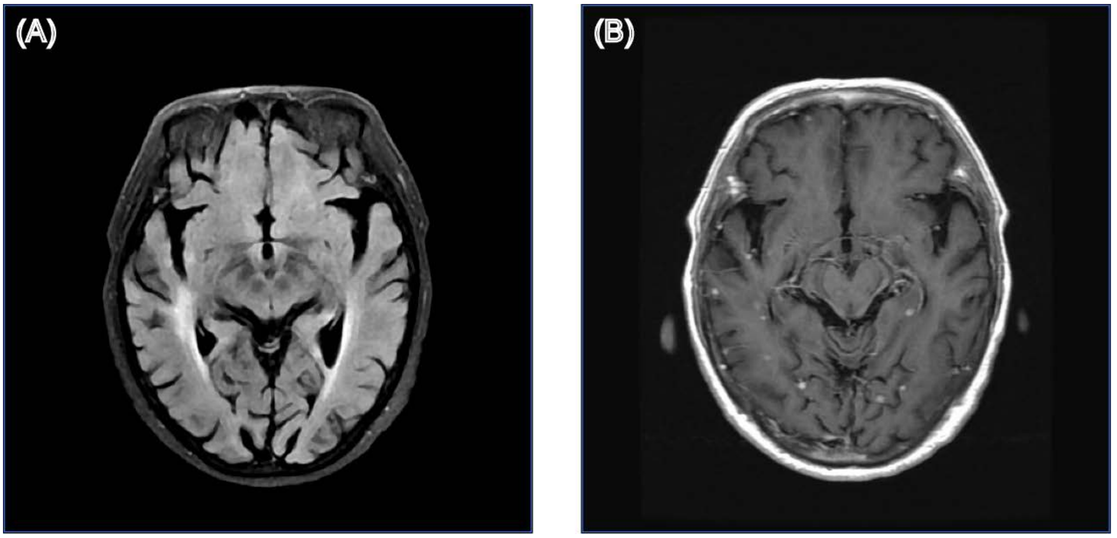

Figure S3 Structural brain MRI images of patient 03. (A) T2-weighted fluid-attenuated inversion recovery (T2-FLAIR) image; (B) Gadolinium-enhanced T1-weighted (Gd-T1w) image.

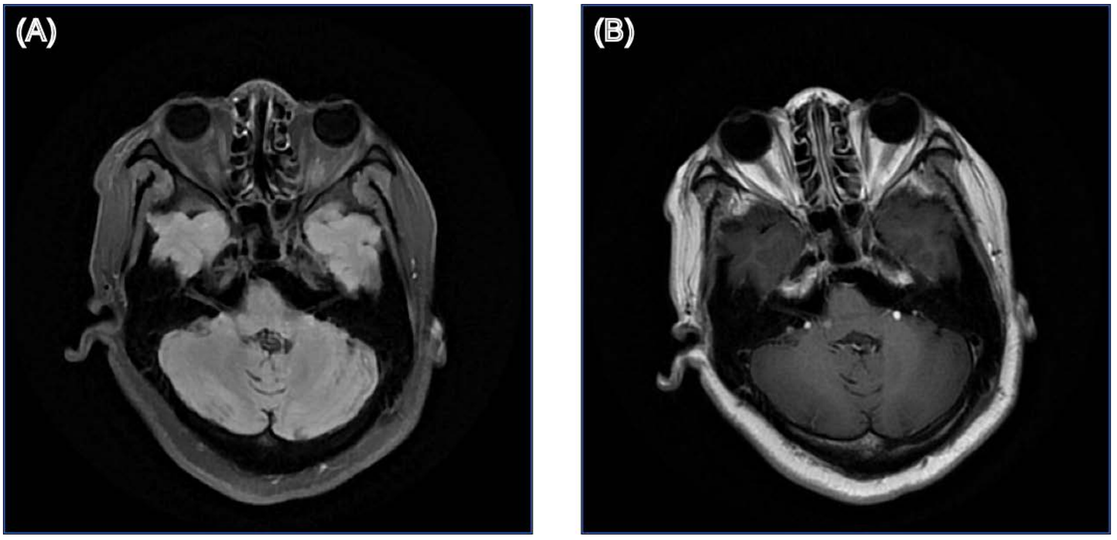

Figure S4 Structural brain MRI images of patient 04. (A) T2-weighted fluid-attenuated inversion recovery (T2-FLAIR) image; (B) Gadolinium-enhanced T1-weighted (Gd-T1w) image.

 https://dx.doi.org/10.21037/qims-22-17

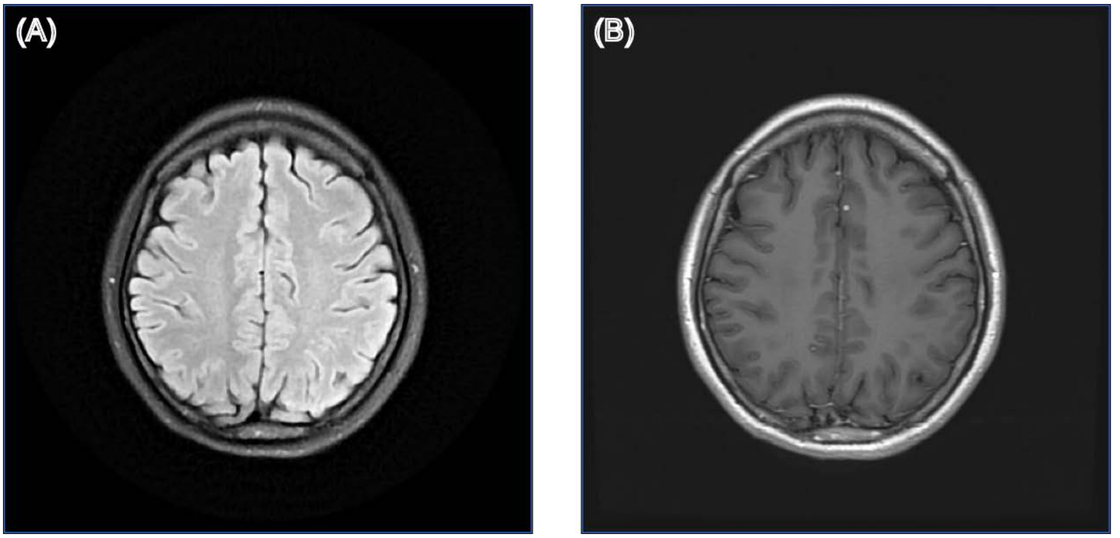

Figure S5 Structural brain MRI images of patient 05. (A) T2-weighted fluid-attenuated inversion recovery (T2-FLAIR) image; (B) Gadolinium-enhanced T1-weighted (Gd-T1w) image.

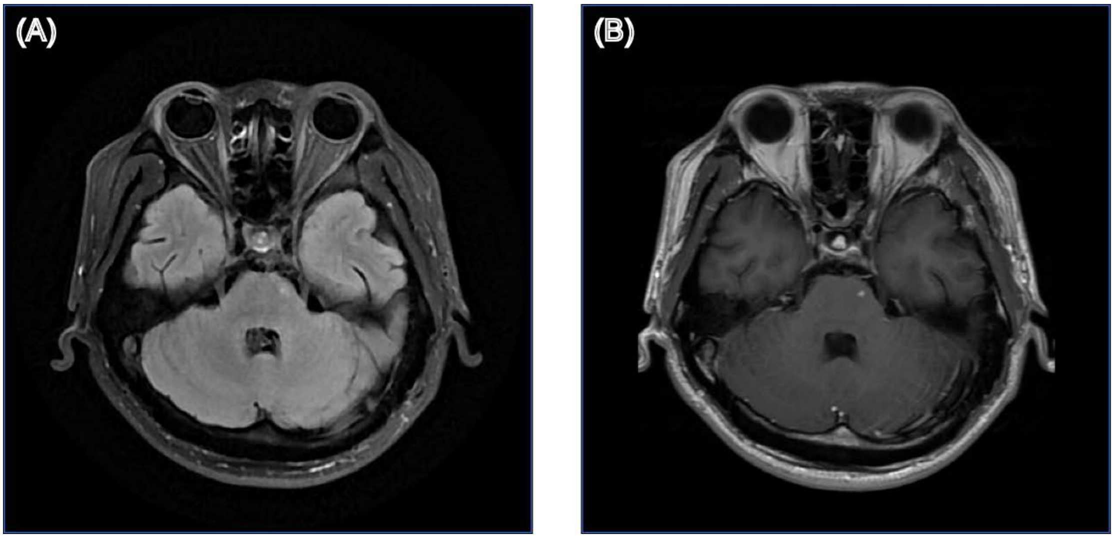

Figure S6 Structural brain MRI images of patient 06. (A) T2-weighted fluid-attenuated inversion recovery (T2-FLAIR) image; (B) Gadolinium-enhanced T1-weighted (Gd-T1w) image.

 https://dx.doi.org/10.21037/qims-22-17

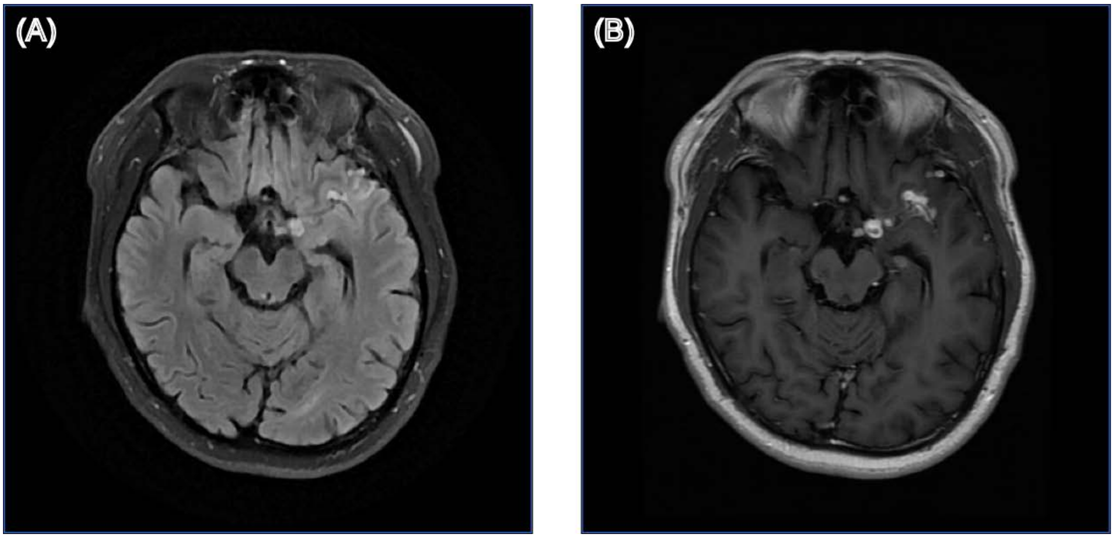

Figure S7 Structural brain MRI images of patient 07. (A) T2-weighted fluid-attenuated inversion recovery (T2-FLAIR) image; (B) Gadolinium-enhanced T1-weighted (Gd-T1w) image.

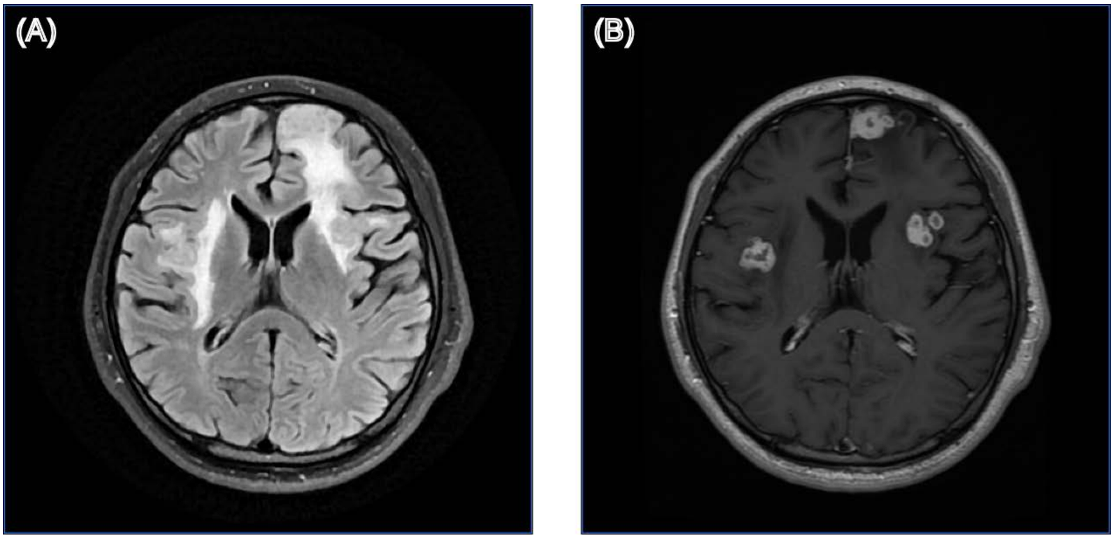

Figure S8 Structural brain MRI images of patient 08. (A) T2-weighted fluid-attenuated inversion recovery (T2-FLAIR) image; (B) Gadolinium-enhanced T1-weighted (Gd-T1w) image.

 https://dx.doi.org/10.21037/qims-22-17

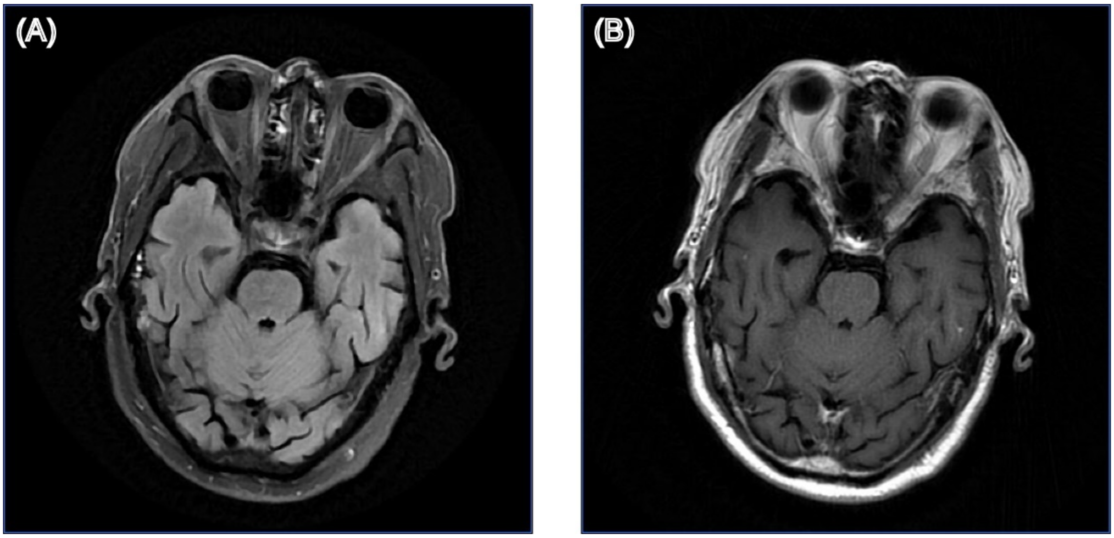

Figure S9 Structural brain MRI images of patient 09. (A) T2-weighted fluid-attenuated inversion recovery (T2-FLAIR) image; (B) Gadolinium-enhanced T1-weighted (Gd-T1w) image.

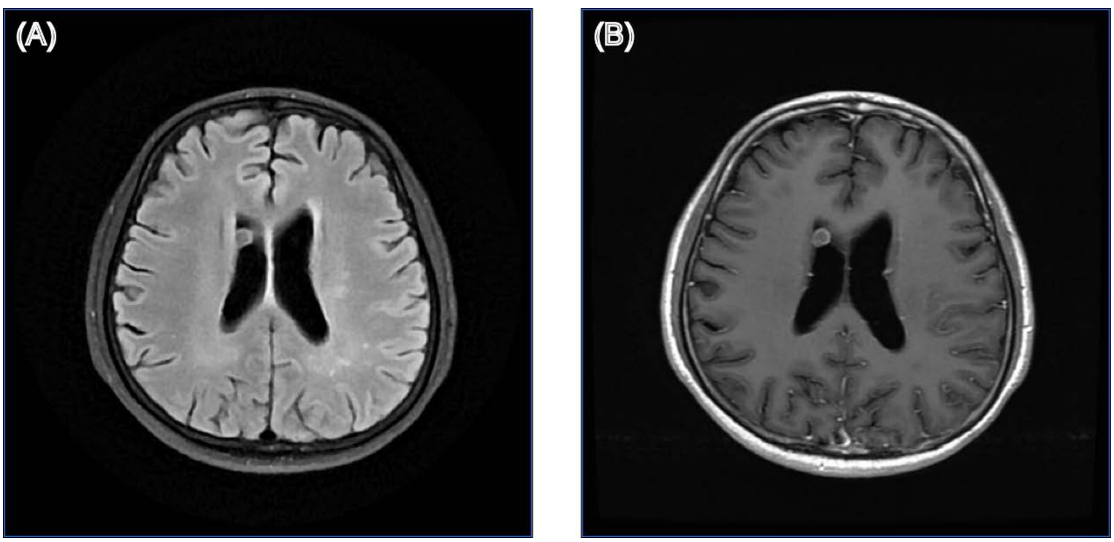

Figure S10 Structural brain MRI images of patient 10. (A) T2-weighted fluid-attenuated inversion recovery (T2-FLAIR) image; (B) Gadolinium-enhanced T1-weighted (Gd-T1w) image.

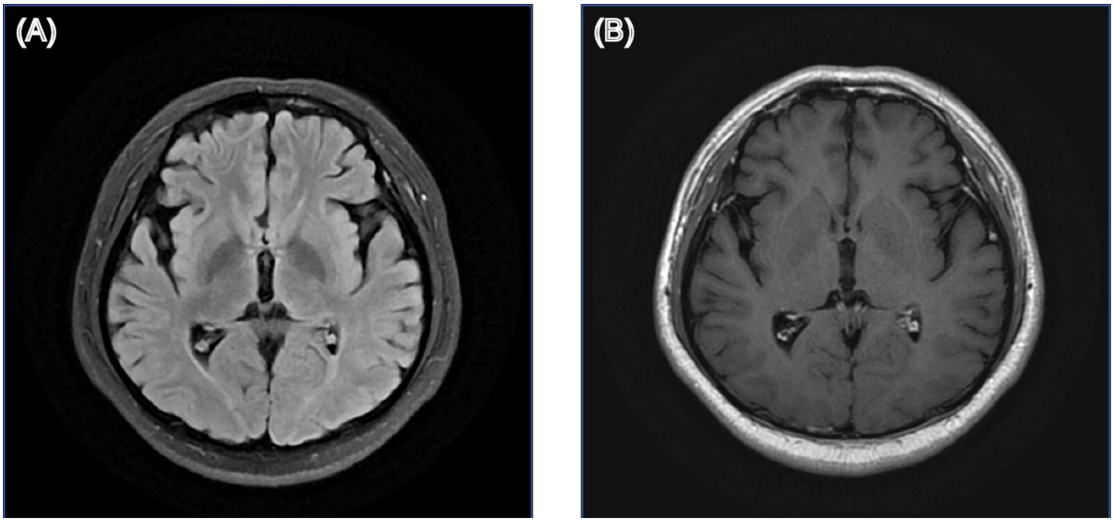

Figure S11 Structural brain MRI images of patient 11. (A) T2-weighted fluid-attenuated inversion recovery (T2-FLAIR) image; (B) Gadolinium-enhanced T1-weighted (Gd-T1w) image.

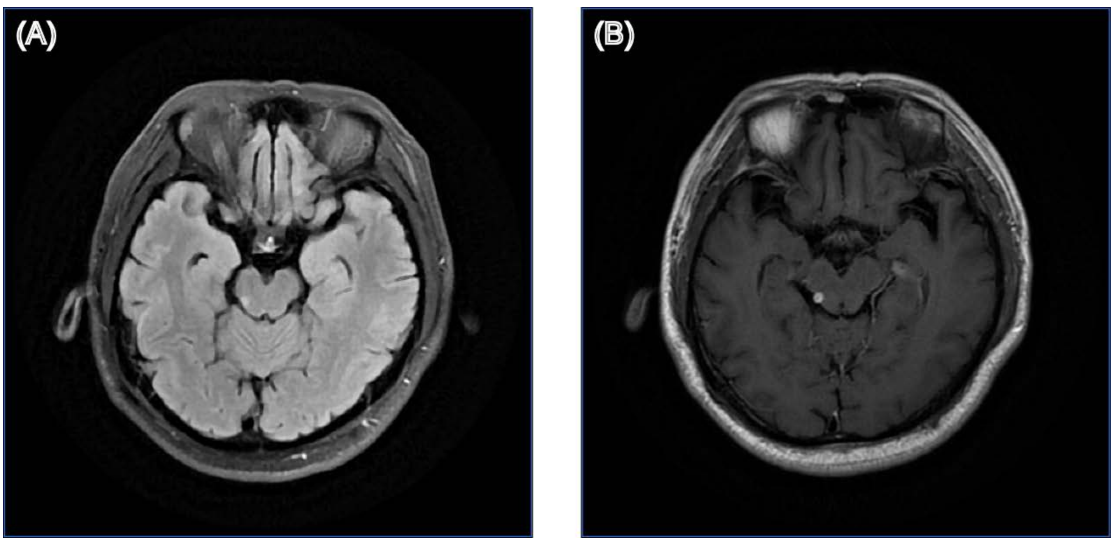

Figure S12 Structural brain MRI images of patient 12. (A) T2-weighted fluid-attenuated inversion recovery (T2-FLAIR) image; (B) Gadolinium-enhanced T1-weighted (Gd-T1w) image.

 https://dx.doi.org/10.21037/qims-22-17

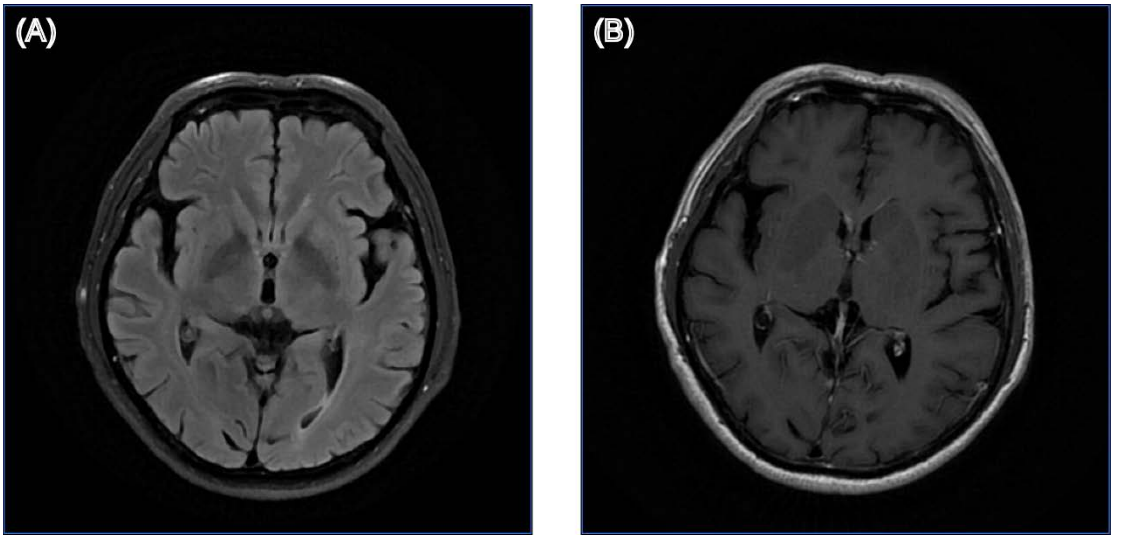

Figure S13 Structural brain MRI images of patient 13. (A) T2-weighted fluid-attenuated inversion recovery (T2-FLAIR) image; (B) Gadolinium-enhanced T1-weighted (Gd-T1w) image.

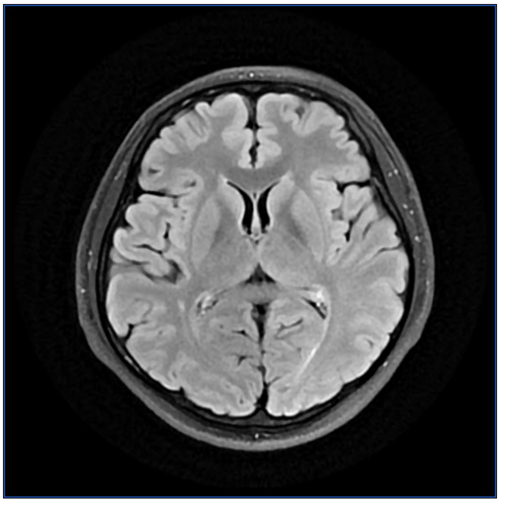

Figure S14 T2-weighted fluid-attenuated inversion recovery (T2-FLAIR) image of patient 14.

 https://dx.doi.org/10.21037/qims-22-17

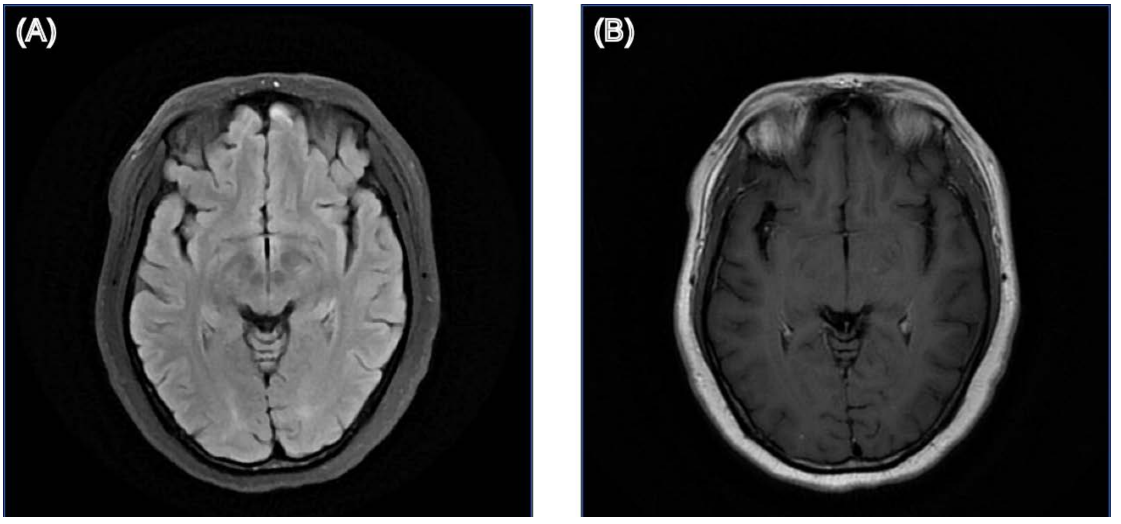

Figure S15 Structural brain MRI images of patient 15. (A) T2-weighted fluid-attenuated inversion recovery (T2-FLAIR) image; (B) Gadolinium-enhanced T1-weighted (Gd-T1w) image.

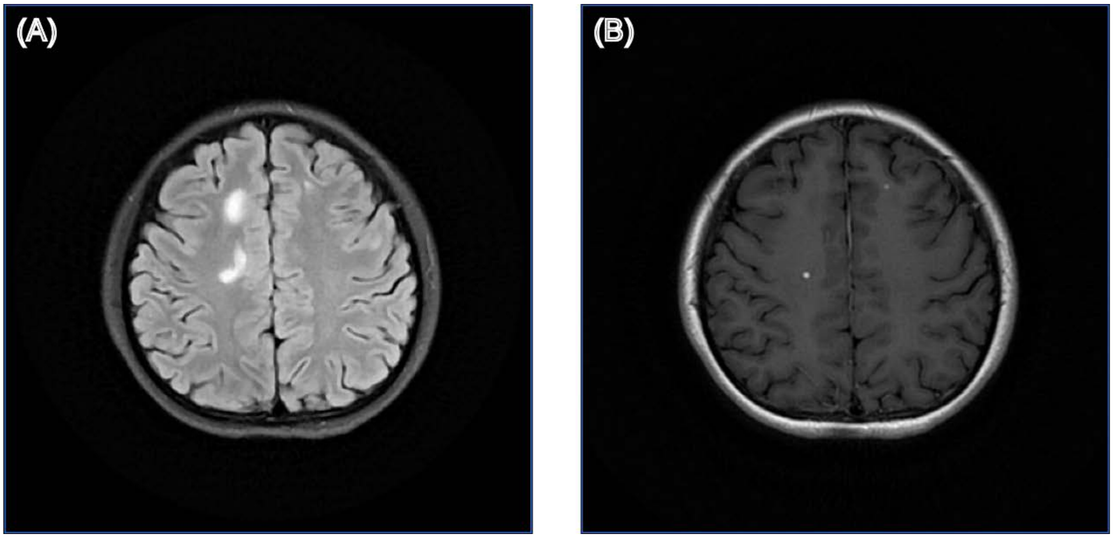

Figure S16 Structural brain MRI images of patient 16. (A) T2-weighted fluid-attenuated inversion recovery (T2-FLAIR) image; (B) Gadolinium-enhanced T1-weighted (Gd-T1w) image.

 https://dx.doi.org/10.21037/qims-22-17

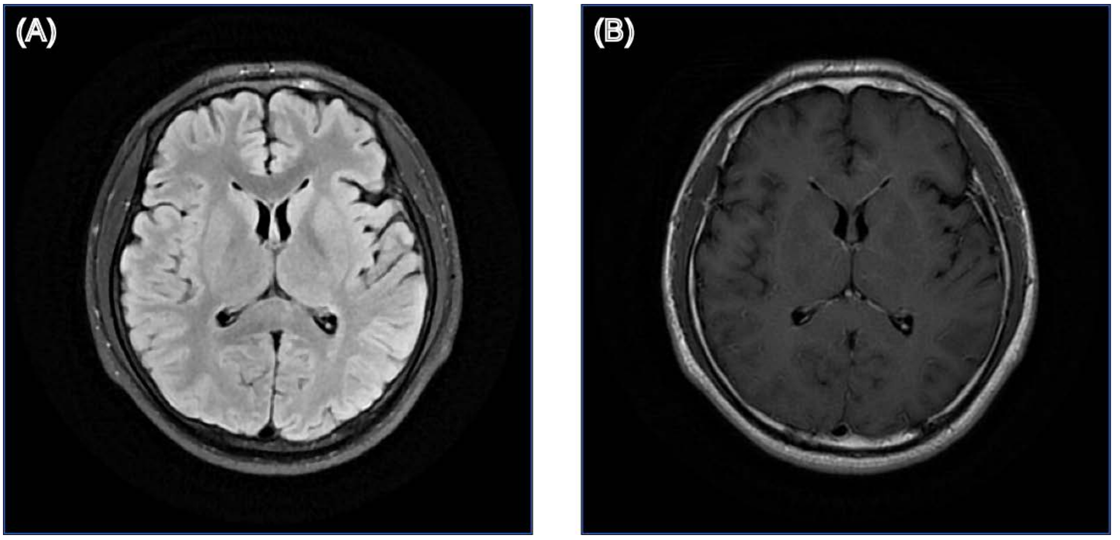

Figure S17 Structural brain MRI images of patient 17. (A) T2-weighted fluid-attenuated inversion recovery (T2-FLAIR) image; (B) Gadolinium-enhanced T1-weighted (Gd-T1w) image.

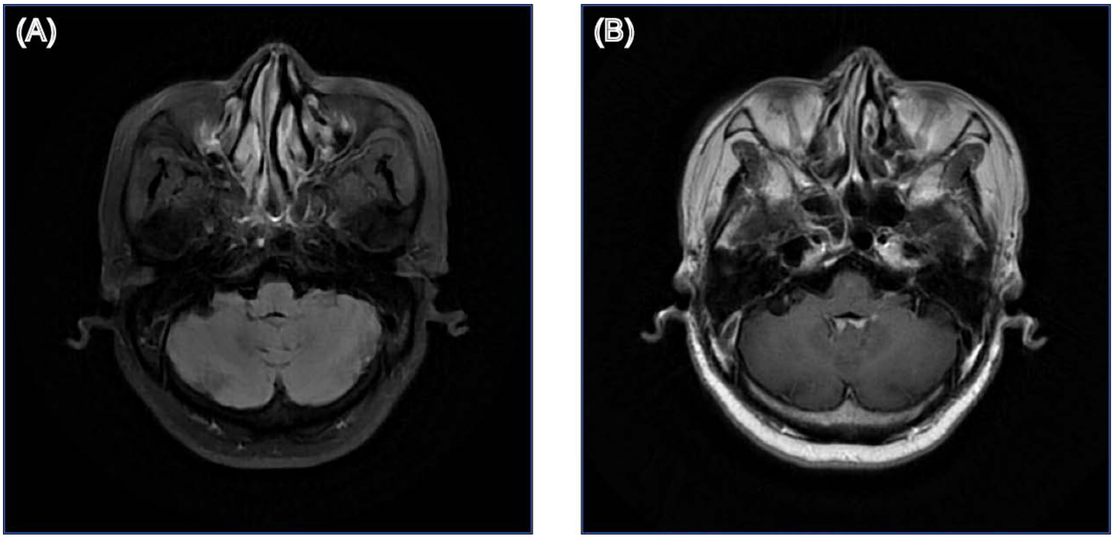

Figure S18 Structural brain MRI images of patient 18. (A) T2-weighted fluid-attenuated inversion recovery (T2-FLAIR) image; (B) Gadolinium-enhanced T1-weighted (Gd-T1w) image.

 https://dx.doi.org/10.21037/qims-22-17

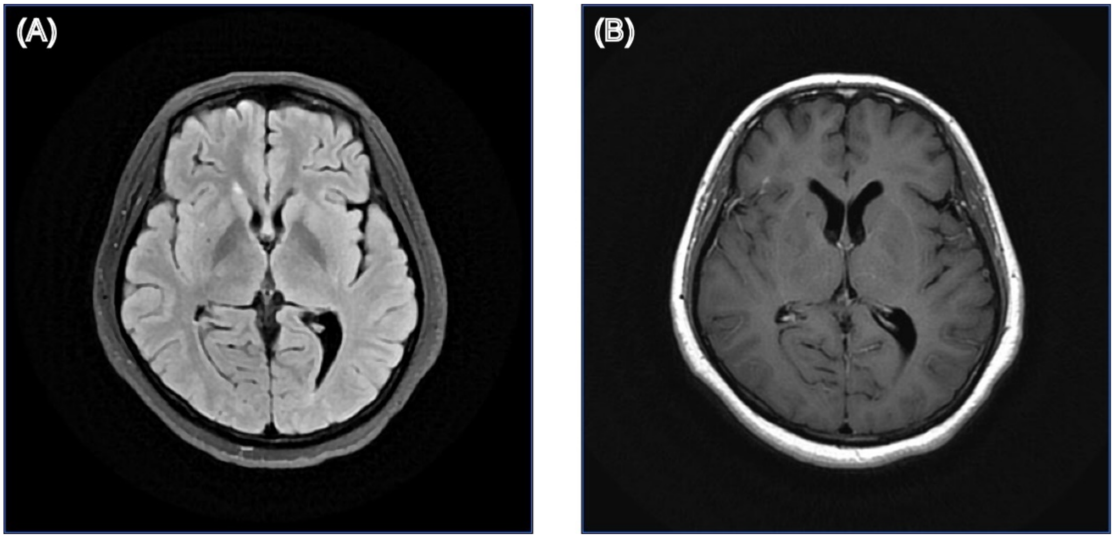

Figure S19 Structural brain MRI images of patient 19. (A) T2-weighted fluid-attenuated inversion recovery (T2-FLAIR) image; (B) Gadolinium-enhanced T1-weighted (Gd-T1w) image.

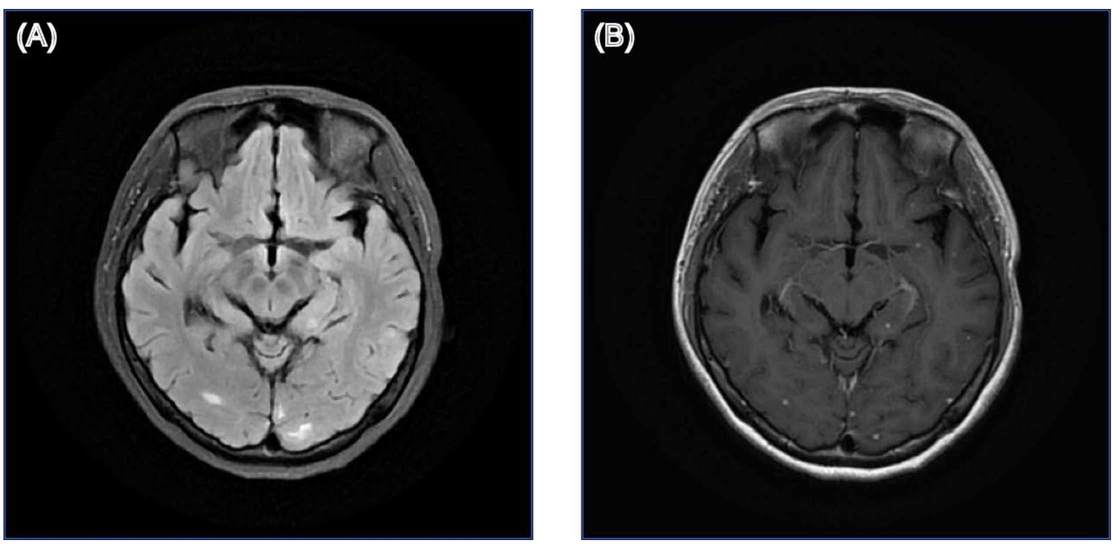

Figure S20 Structural brain MRI images of patient 20. (A) T2-weighted fluid-attenuated inversion recovery (T2-FLAIR) image; (B) Gadolinium-enhanced T1-weighted (Gd-T1w) image.

 https://dx.doi.org/10.21037/qims-22-17

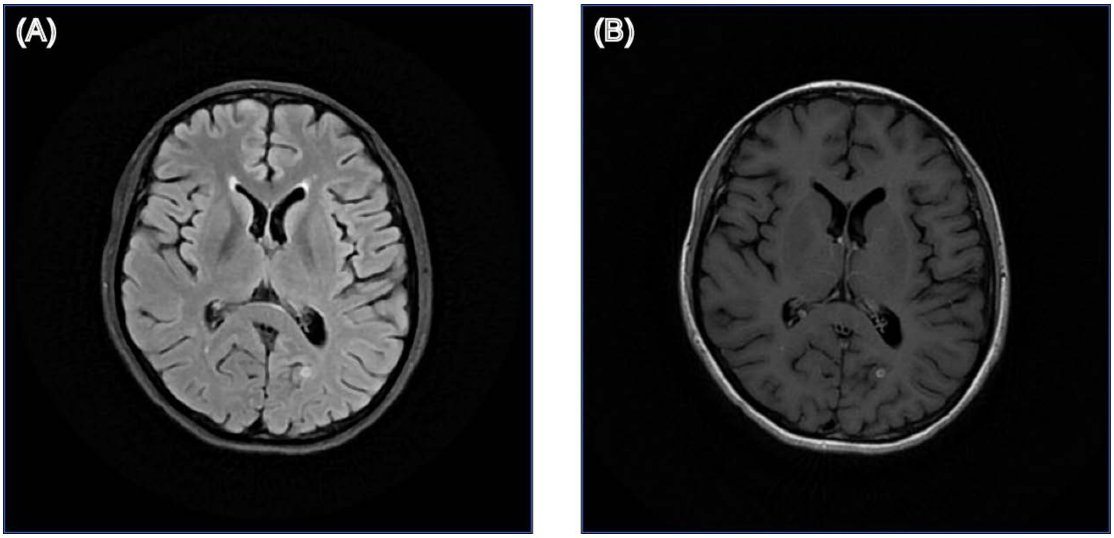

Figure S21 Structural brain MRI images of patient 21. (A) T2-weighted fluid-attenuated inversion recovery (T2-FLAIR) image; (B) Gadolinium-enhanced T1-weighted (Gd-T1w) image.

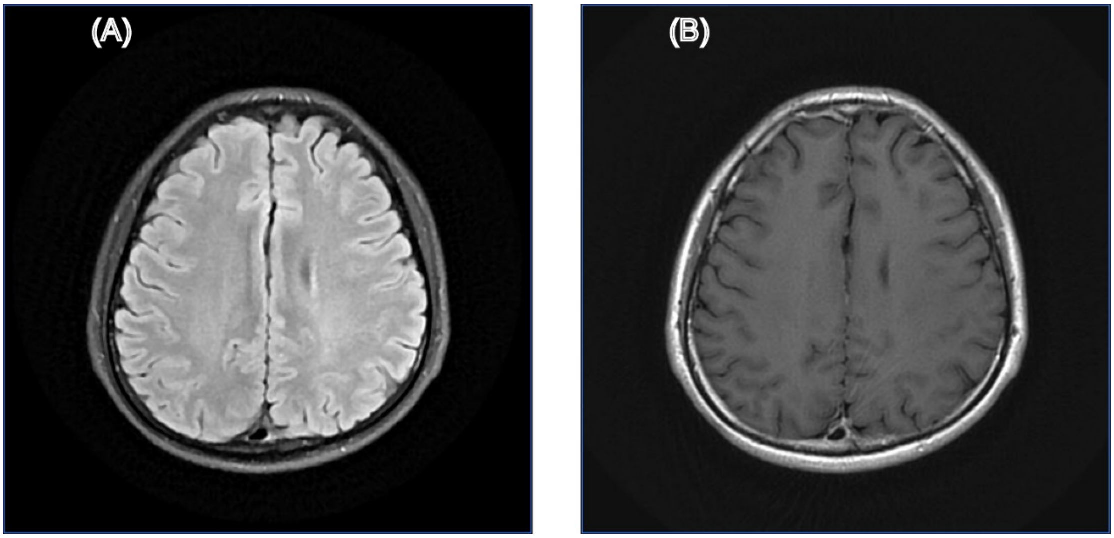

Figure S22 Structural brain MRI images of patient 22. (A) T2-weighted fluid-attenuated inversion recovery (T2-FLAIR) image; (B) Gadolinium-enhanced T1-weighted (Gd-T1w) image.

 https://dx.doi.org/10.21037/qims-22-17

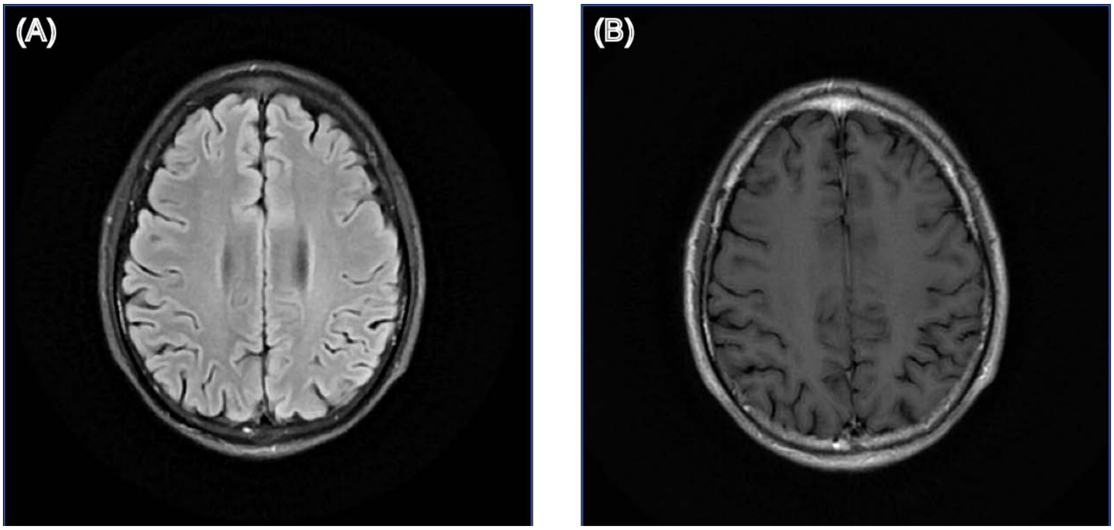

Figure S23 Structural brain MRI images of patient 23. (A) T2-weighted fluid-attenuated inversion recovery (T2-FLAIR) image; (B) Gadolinium-enhanced T1-weighted (Gd-T1w) image.

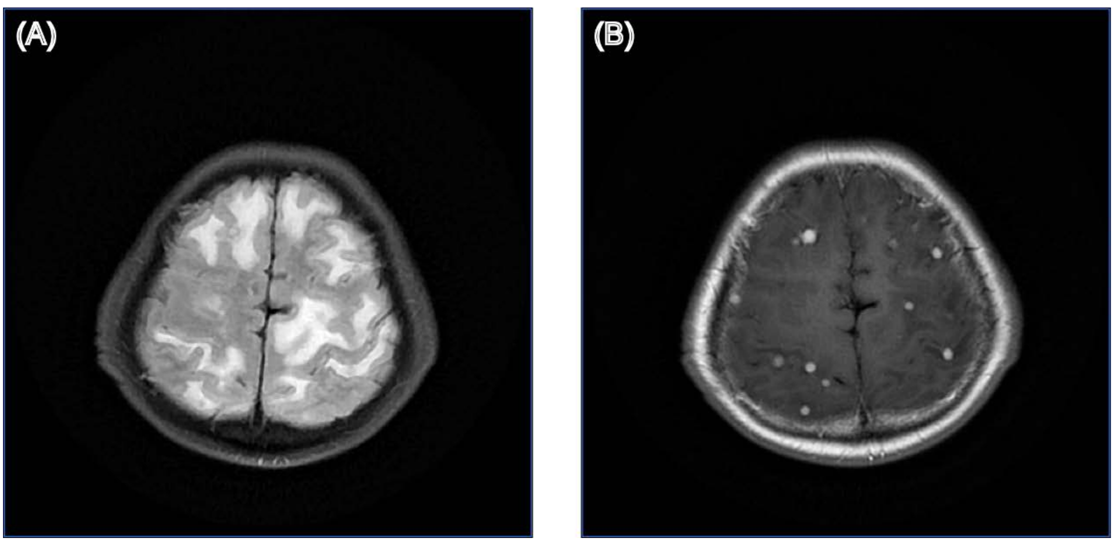

Figure S24 Structural brain MRI images of patient 24. (A) T2-weighted fluid-attenuated inversion recovery (T2-FLAIR) image; (B) Gadolinium-enhanced T1-weighted (Gd-T1w) image.

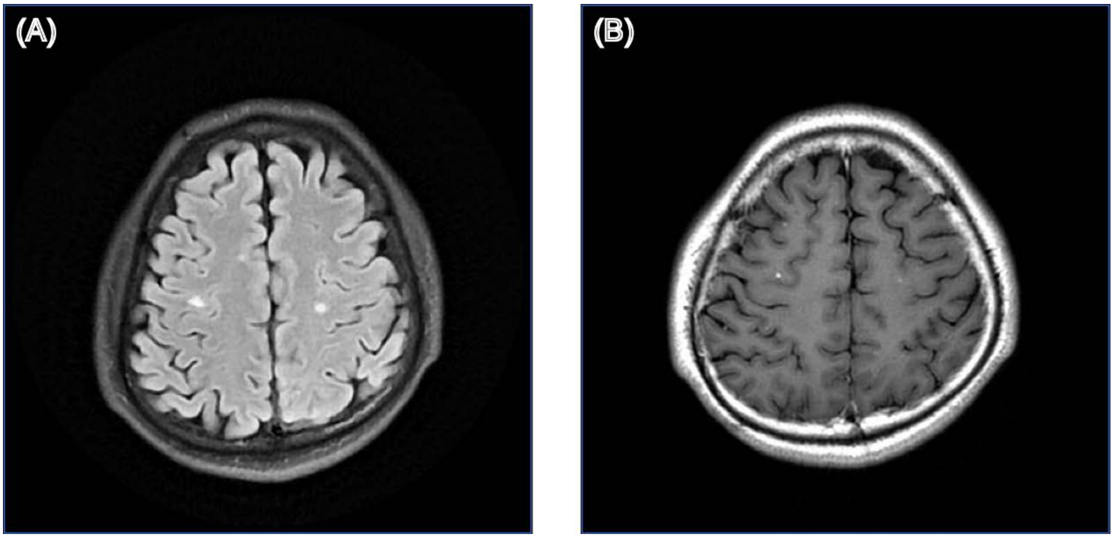

Figure S25 Structural brain MRI images of patient 25. (A) T2-weighted fluid-attenuated inversion recovery (T2-FLAIR) image; (B) Gadolinium-enhanced T1-weighted (Gd-T1w) image.

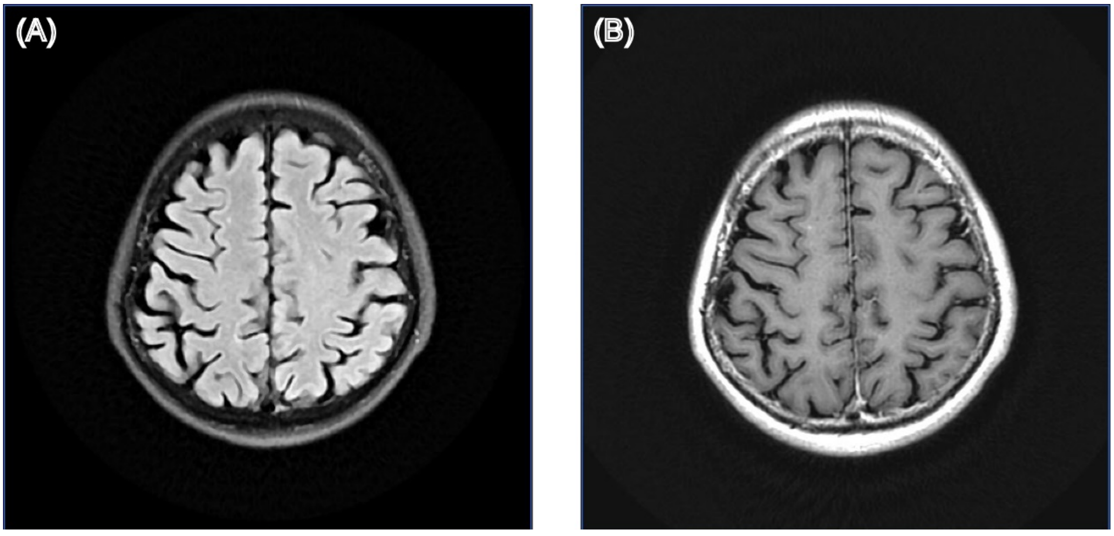

Figure S26 Structural brain MRI images of patient 26. (A) T2-weighted fluid-attenuated inversion recovery (T2-FLAIR) image; (B) Gadolinium-enhanced T1-weighted (Gd-T1w) image.

 https://dx.doi.org/10.21037/qims-22-17

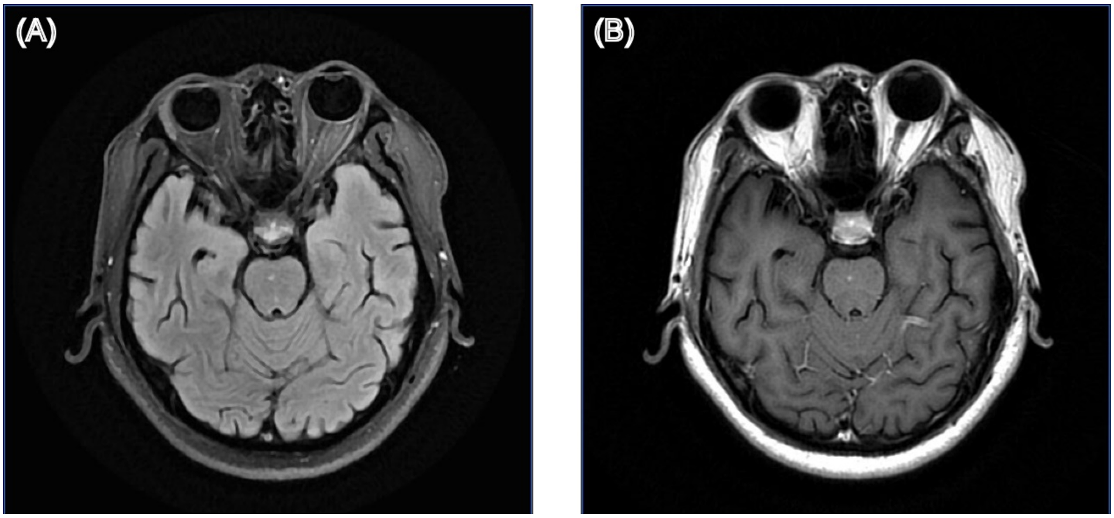

Figure S27 Structural brain MRI images of patient 27. (A) T2-weighted fluid-attenuated inversion recovery (T2-FLAIR) image; (B) Gadolinium-enhanced T1-weighted (Gd-T1w) image.

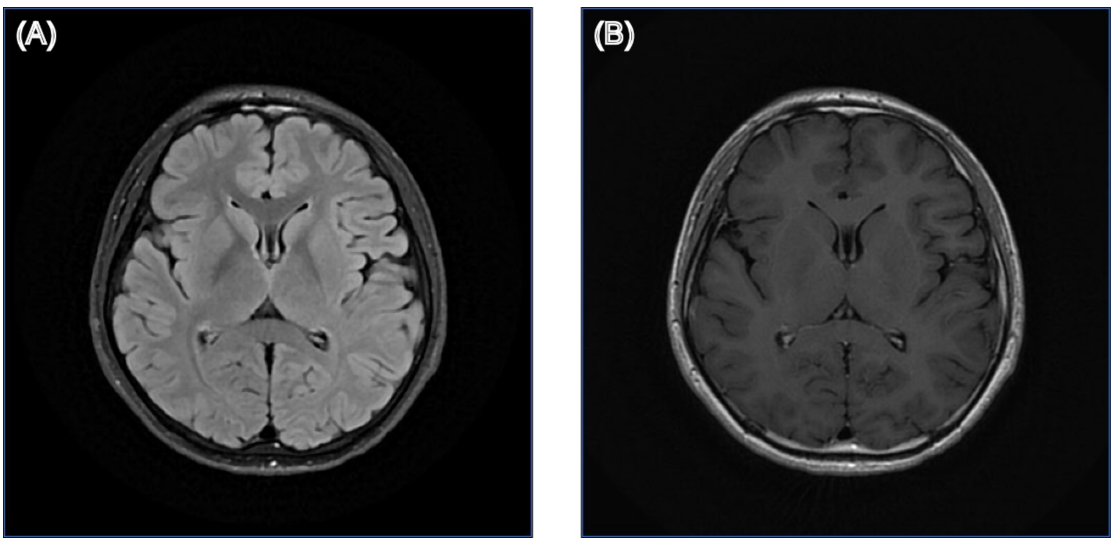

Figure S28 Structural brain MRI images of patient 28. (A) T2-weighted fluid-attenuated inversion recovery (T2-FLAIR) image; (B) Gadolinium-enhanced T1-weighted (Gd-T1w) image.

 https://dx.doi.org/10.21037/qims-22-17

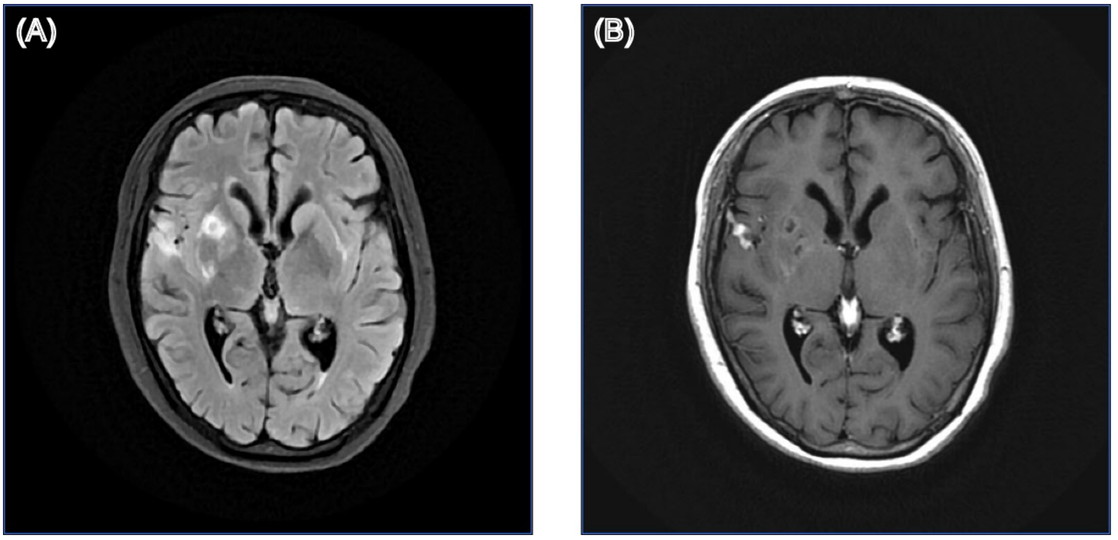

Figure S29 Structural brain MRI images of patient 29. (A) T2-weighted fluid-attenuated inversion recovery (T2-FLAIR) image; (B) Gadolinium-enhanced T1-weighted (Gd-T1w) image.

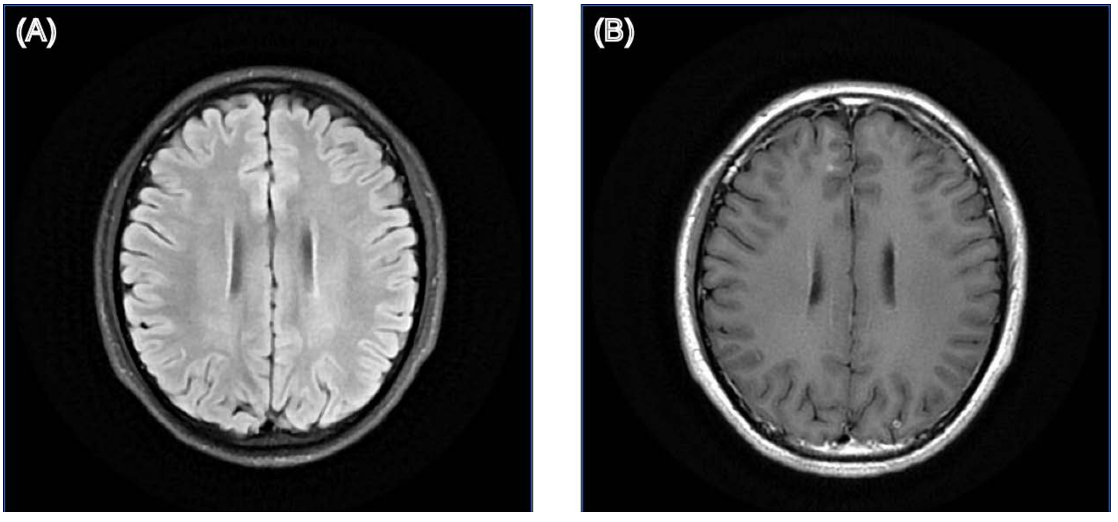

Figure S30 Structural brain MRI images of patient 30. (A) T2-weighted fluid-attenuated inversion recovery (T2-FLAIR) image; (B) Gadolinium-enhanced T1-weighted (Gd-T1w) image.

 https://dx.doi.org/10.21037/qims-22-17

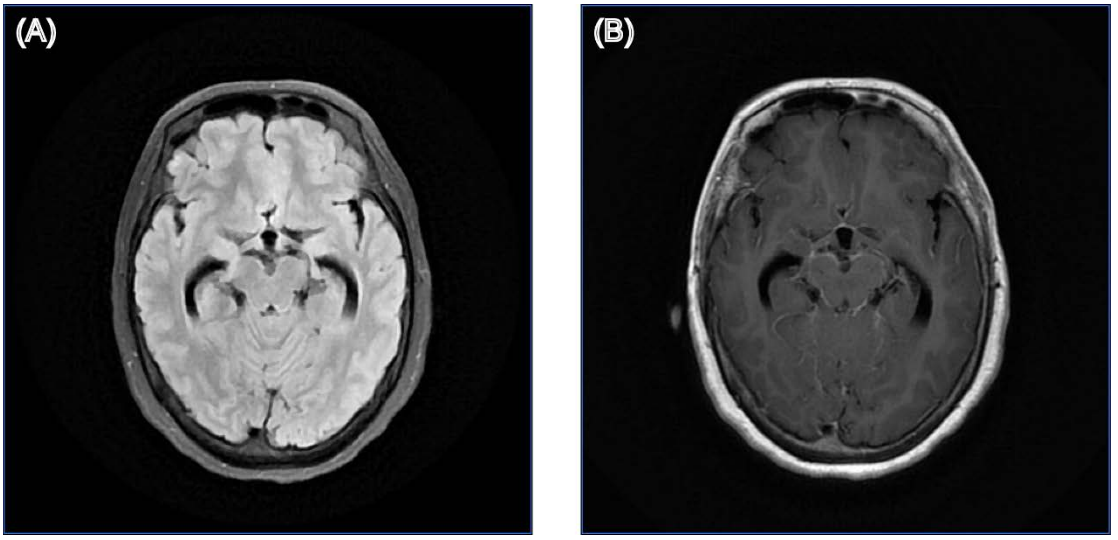

Figure S31 Structural brain MRI images of patient 31. (A) T2-weighted fluid-attenuated inversion recovery (T2-FLAIR) image; (B) Gadolinium-enhanced T1-weighted (Gd-T1w) image.

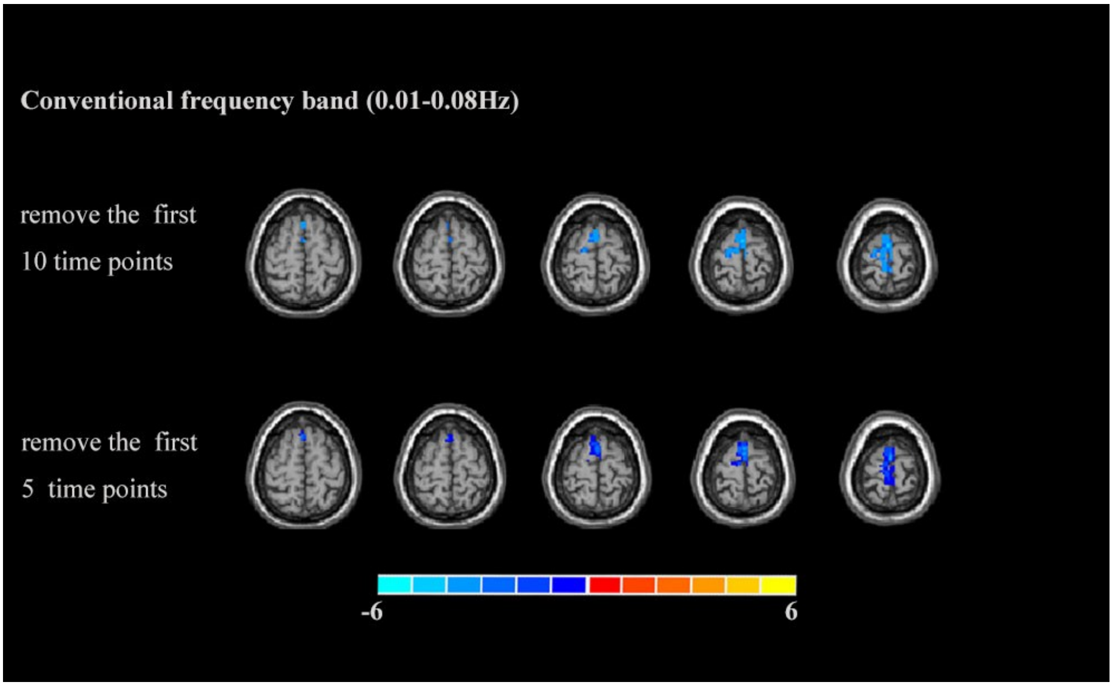

Figure S32 Patterns of ALFF that analyzed with removing the first 10 time points and patterns of results that analyzed with removing the first 5 time points in the conventional frequency band (0.01-0.08 Hz). ALFF, amplitude of low-frequency fluctuation.

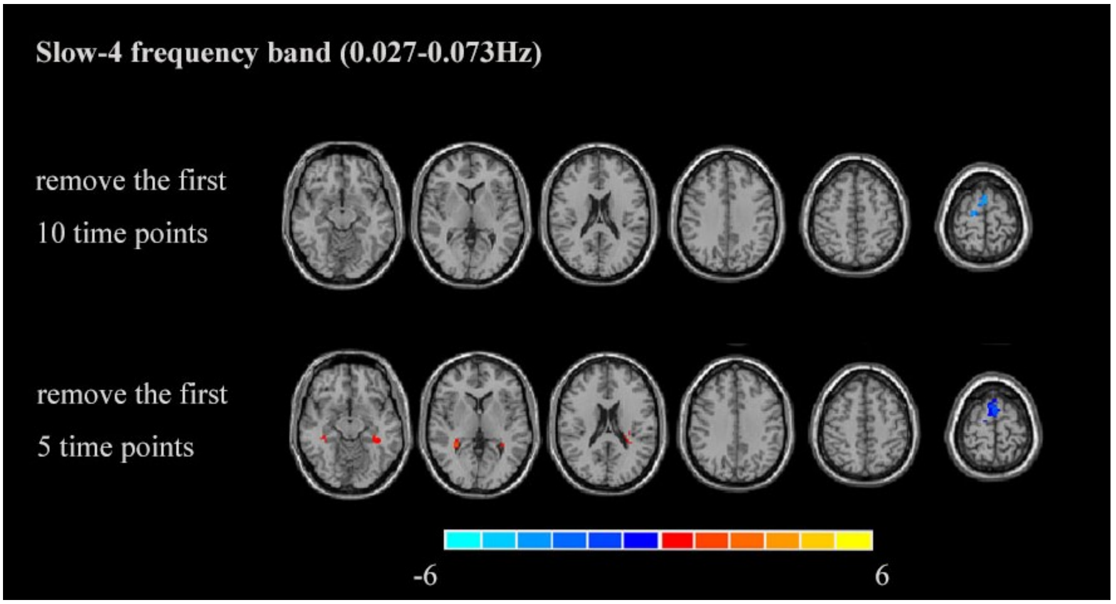

Figure S33 Patterns of ALFF that analyzed with removing the first 10 time points and patterns of results that analyzed with removing the first 5 time points in the slow-4 frequency band (0.027-0.073 Hz). ALFF, amplitude of low-frequency fluctuation.

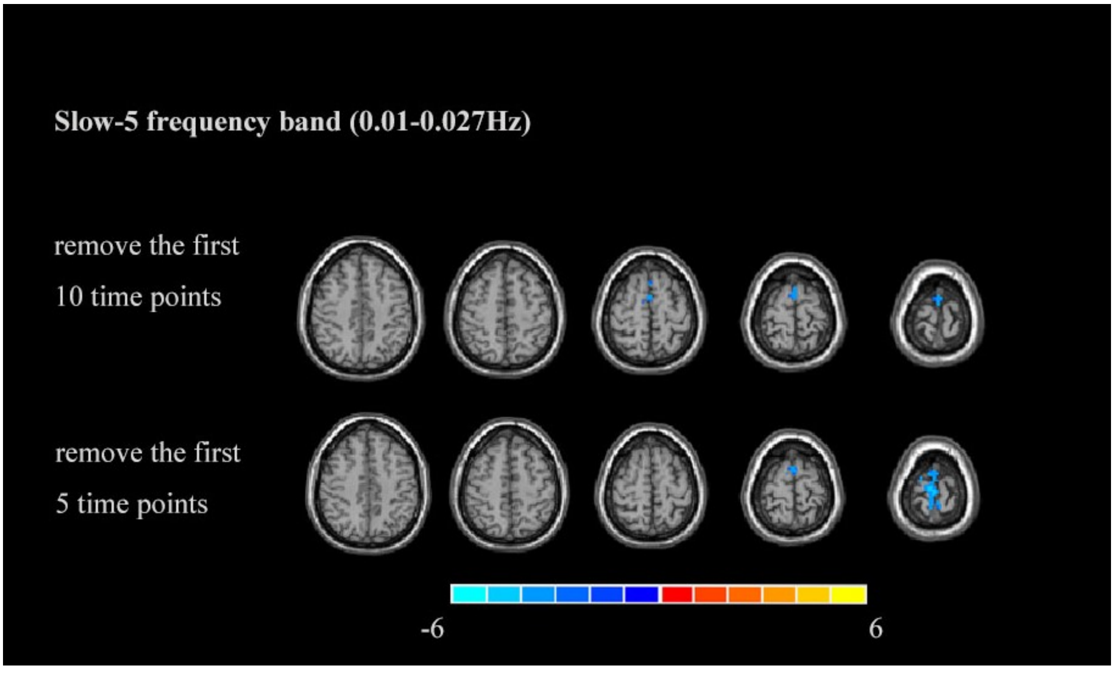

Figure S34 Patterns of ALFF that analyzed with removing the first 10 time points and patterns of results that analyzed with removing the first 5 time points in the slow-5 frequency band (0.01-0.027 Hz). ALFF, amplitude of low-frequency fluctuation.

 https://dx.doi.org/10.21037/qims-22-17

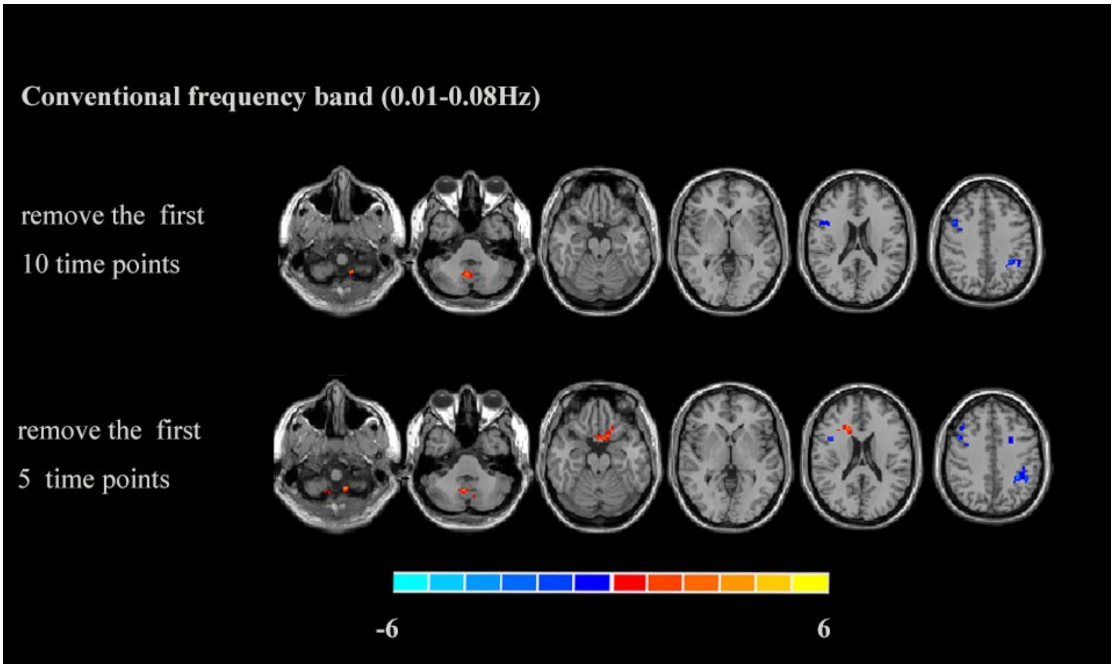

Figure S35 Patterns of fALFF that analyzed with removing the first 10 time points and patterns of results that analyzed with removing the first 5 time points in the conventional frequency band (0.01-0.08 Hz). fALFF, fractional amplitude of low-frequency fluctuation.

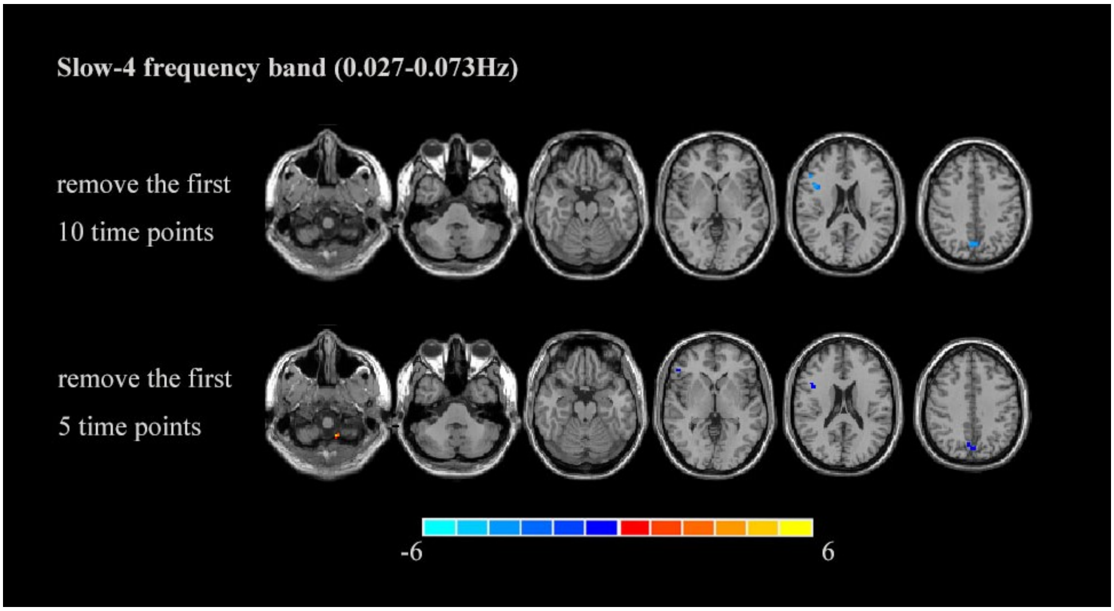

Figure S36 Patterns of fALFF that analyzed with removing the first 10 time points and patterns of results that analyzed with removing the first 5 time points in the slow-4 frequency band (0.027-0.073 Hz). fALFF, fractional amplitude of low-frequency fluctuation.

 https://dx.doi.org/10.21037/qims-22-17

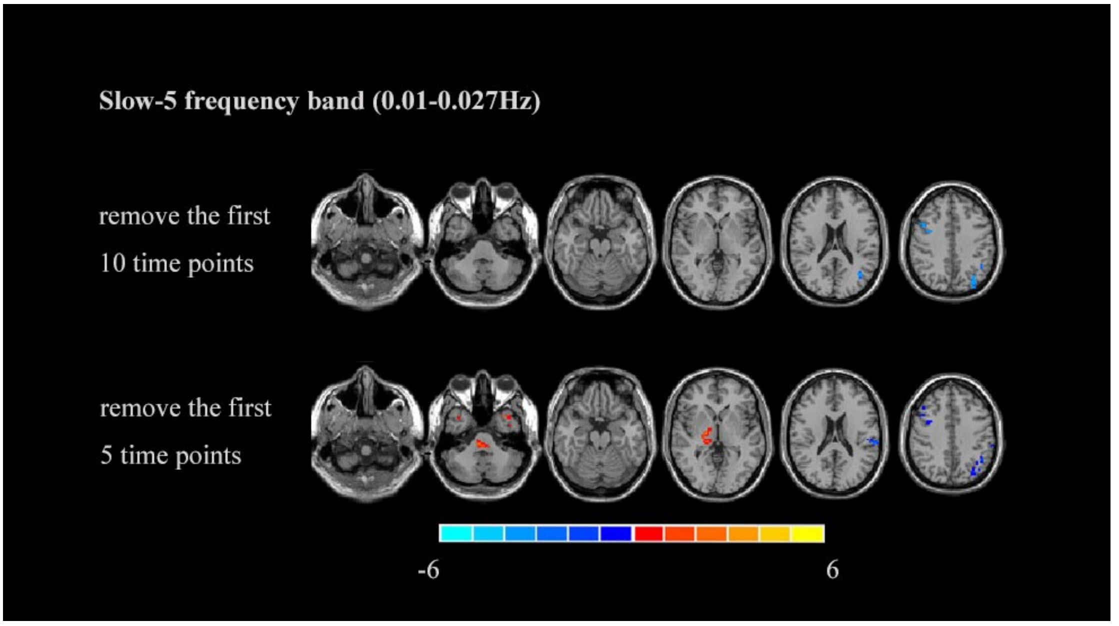

Figure S37 Patterns of fALFF that analyzed with removing the first 10 time points and patterns of results that analyzed with removing the first 5 time points in the slow-5 frequency band (0.01-0.027 Hz). fALFF, fractional amplitude of low-frequency fluctuation.

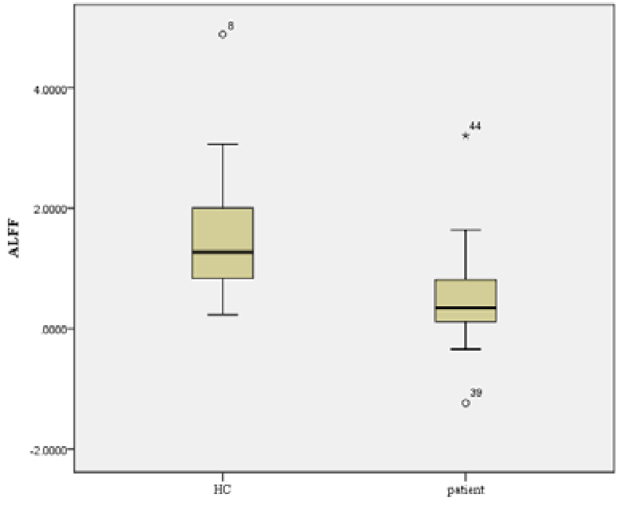

Figure S38 Results of the normality test for ALFF values in the Paracentral_Lobule_R in the conventional frequency band (0.01-0.08 Hz). ALFF, amplitude of low-frequency fluctuation.

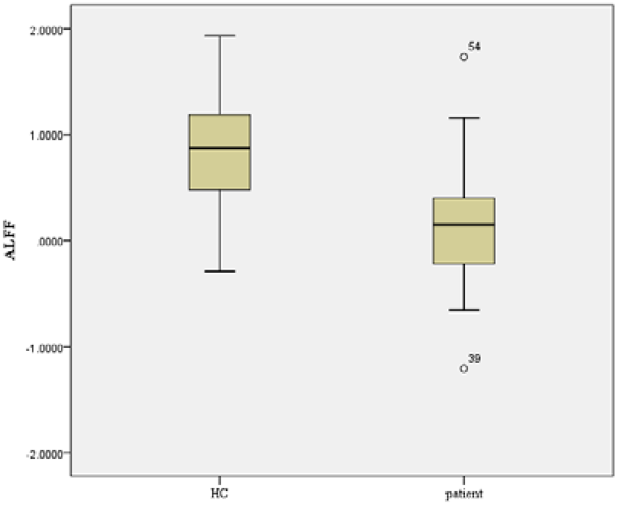

Figure S39 Results of the normality test for ALFF values in the Supp_Motor_Area_R in the slow-4 frequency band (0.027-0.073 Hz). ALFF, amplitude of low-frequency fluctuation.

 https://dx.doi.org/10.21037/qims-22-17

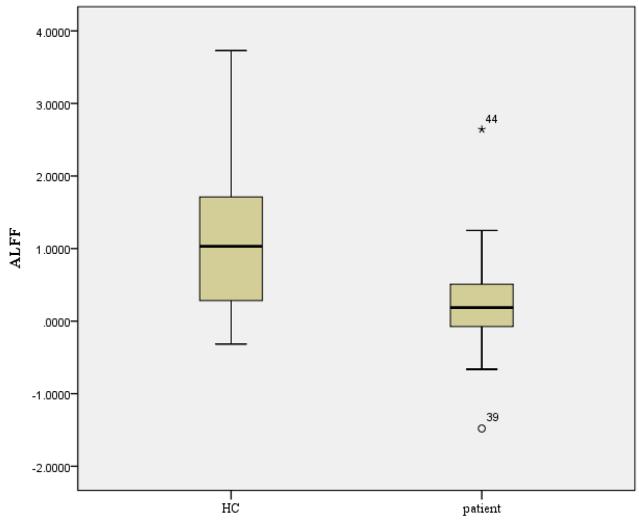

Figure S40 Results of the normality test for ALFF values in the Supp_Motor_Area_L in the slow-5 frequency band (0.01-0.027 Hz). ALFF, amplitude of low-frequency fluctuation.

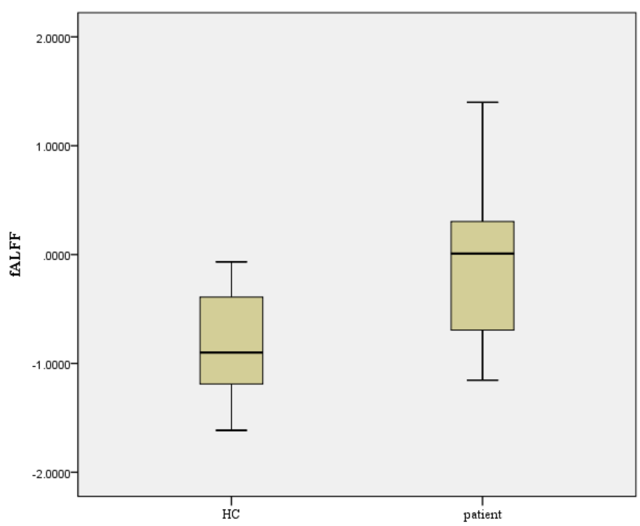

Figure S41 Results of the normality test for fALFF values in the Cerebelum_9_L in the conventional frequency band (0.01-0.08 Hz). fALFF, fractional amplitude of low-frequency fluctuation.

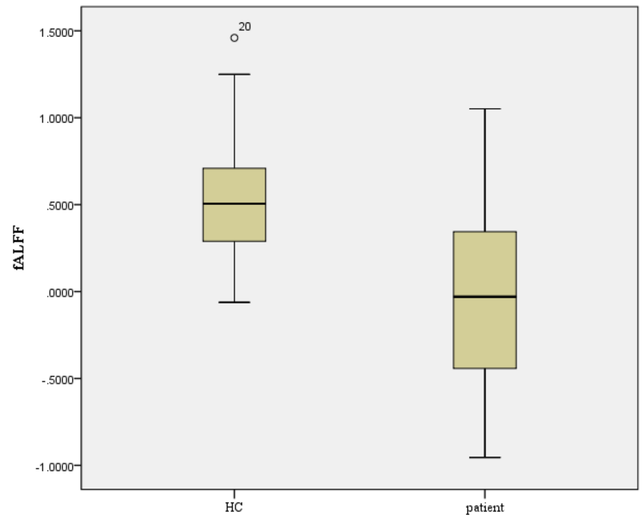

Figure S42 Results of the normality test for fALFF values in the Frontal_Inf_Oper_R in the conventional frequency band (0.01-0.08 Hz). fALFF, fractional amplitude of low-frequency fluctuation.

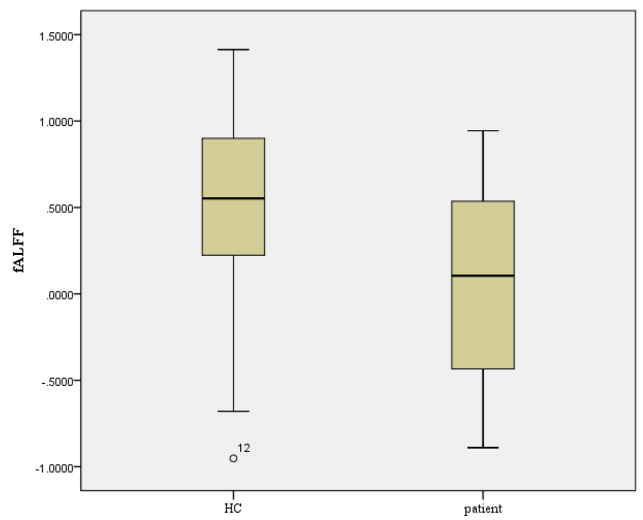

Figure S43 Results of the normality test for fALFF values in the Parietal_Inf_L in the conventional frequency band (0.01-0.08 Hz). fALFF, fractional amplitude of low-frequency fluctuation.

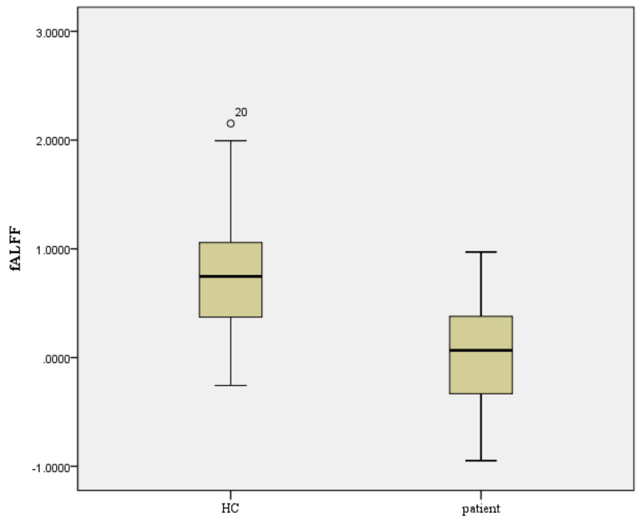

Figure S44 Results of the normality test for fALFF values in the Frontal_Inf_Oper_R in the slow-4 frequency band (0.027-0.073 Hz). fALFF, fractional amplitude of low-frequency fluctuation.

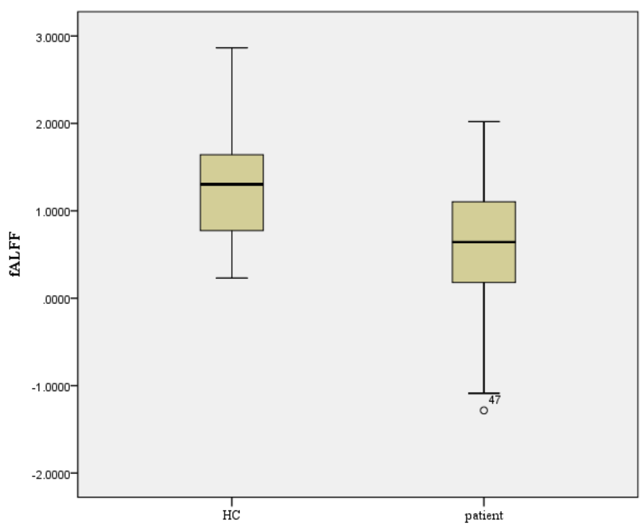

Figure S45 Results of the normality test for fALFF values in the Precuneus_R in the slow-4 frequency band (0.027-0.073 Hz). fALFF, fractional amplitude of low-frequency fluctuation.

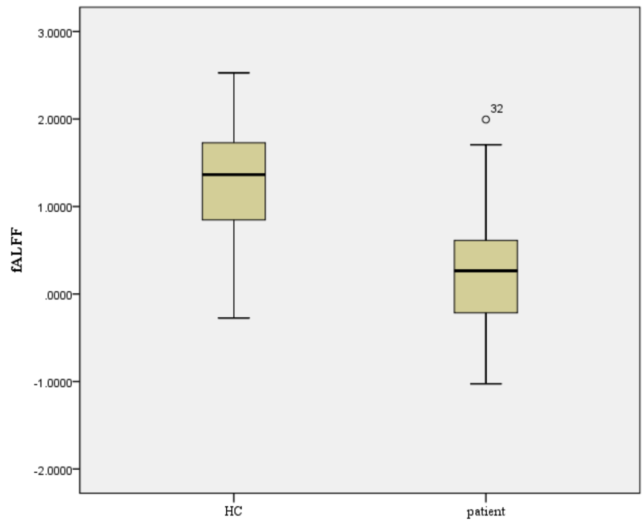

Figure S46 Results of the normality test for fALFF values in the Occipital_Mid_L in the slow-5 frequency band (0.01-0.027 Hz). fALFF, fractional amplitude of low-frequency fluctuation.

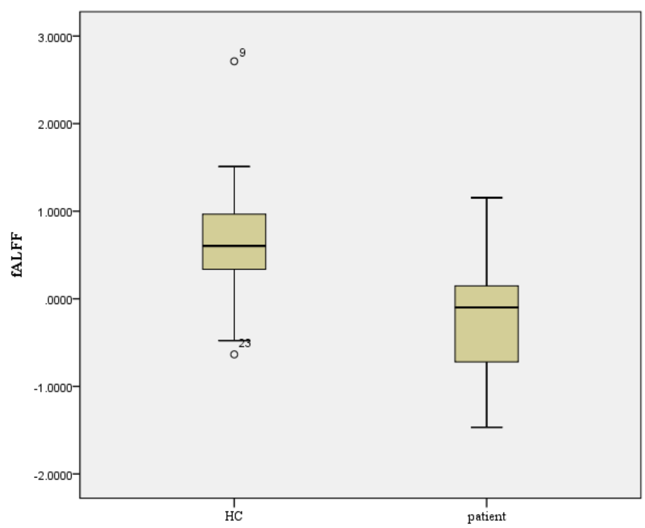

Figure S47 Results of the normality test for fALFF values in the Frontal_Mid_R in the slow-5 frequency band (0.01-0.027 Hz). fALFF, fractional amplitude of low-frequency fluctuation.

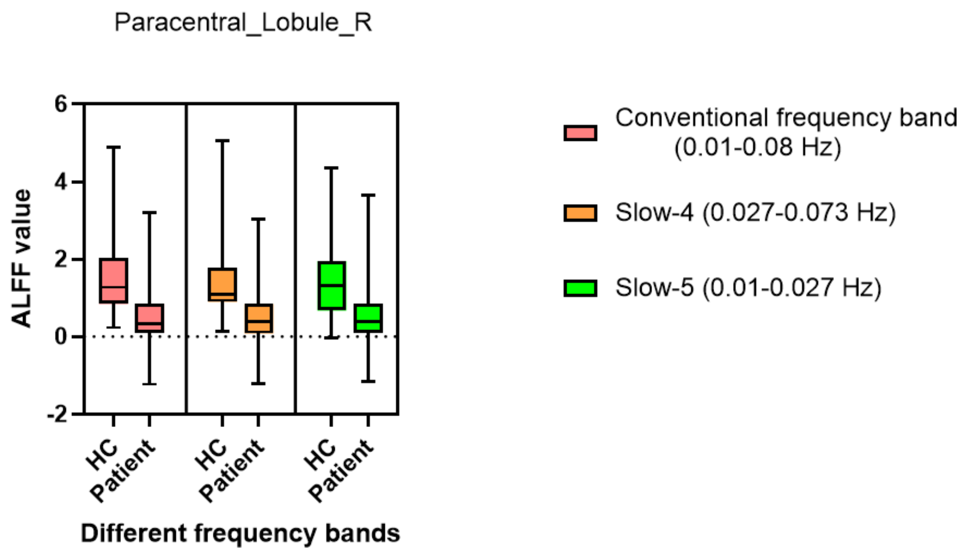

Figure S48 The ALFF value of Paracentral_Lobule_R in different frequency bands. ALFF, amplitude of low-frequency fluctuation.

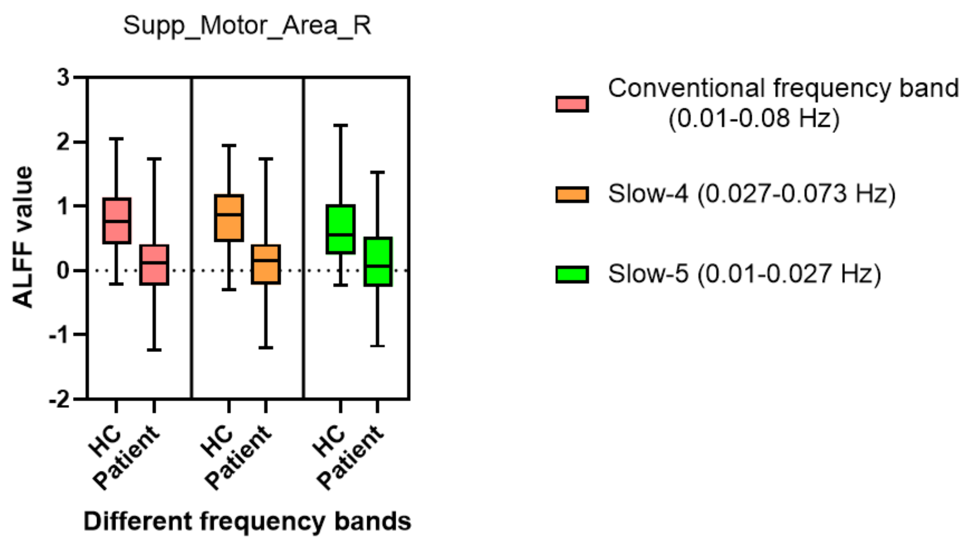

Figure S49 The ALFF value of Supp_Motor_Area_R in different frequency bands. ALFF, amplitude of low-frequency fluctuation.

 https://dx.doi.org/10.21037/qims-22-17

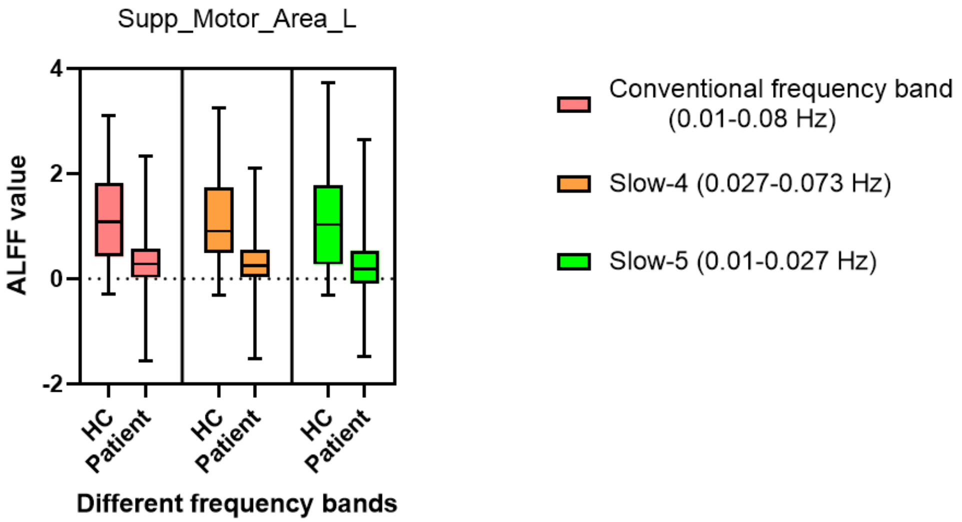

Figure S50 The ALFF value of Supp_Motor_Area_L in different frequency bands. ALFF, amplitude of low-frequency fluctuation.

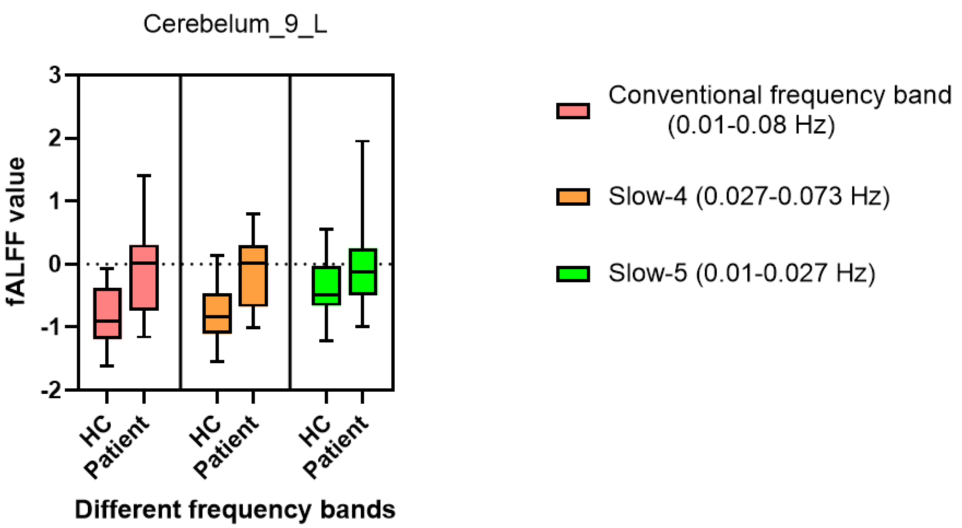

Figure S51 The fALFF value of Cerebelum_9_L in different frequency bands. fALFF, fractional amplitude of low-frequency fluctuation.

 https://dx.doi.org/10.21037/qims-22-17

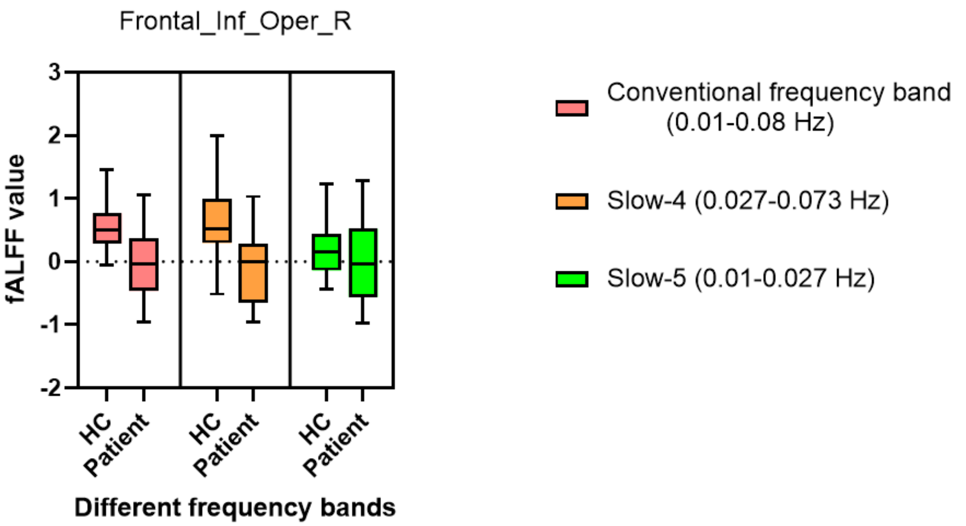

Figure S52 The fALFF value of Frontal_Inf_Oper_R in different frequency bands. fALFF, fractional amplitude of low-frequency fluctuation.

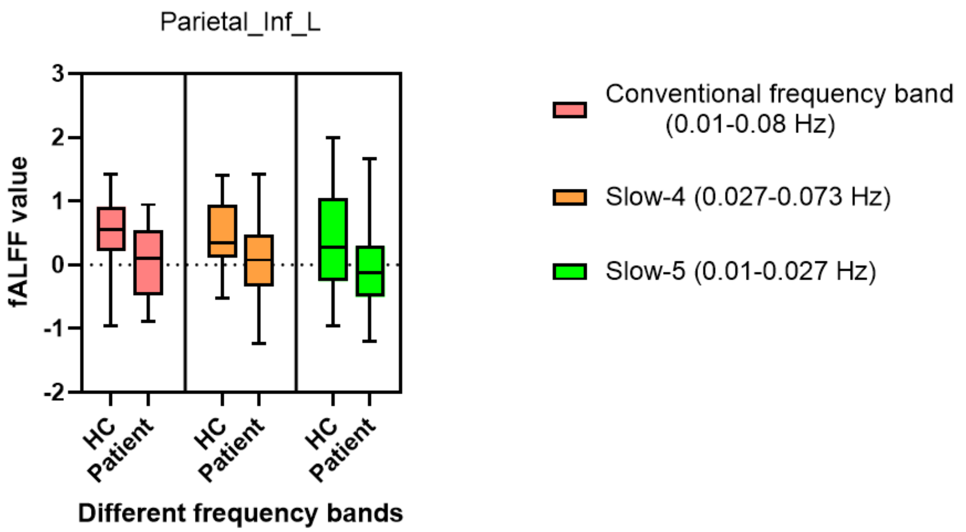

Figure S53 The fALFF value of Parietal_Inf_L in different frequency bands. fALFF, fractional amplitude of low-frequency fluctuation.

 https://dx.doi.org/10.21037/qims-22-17

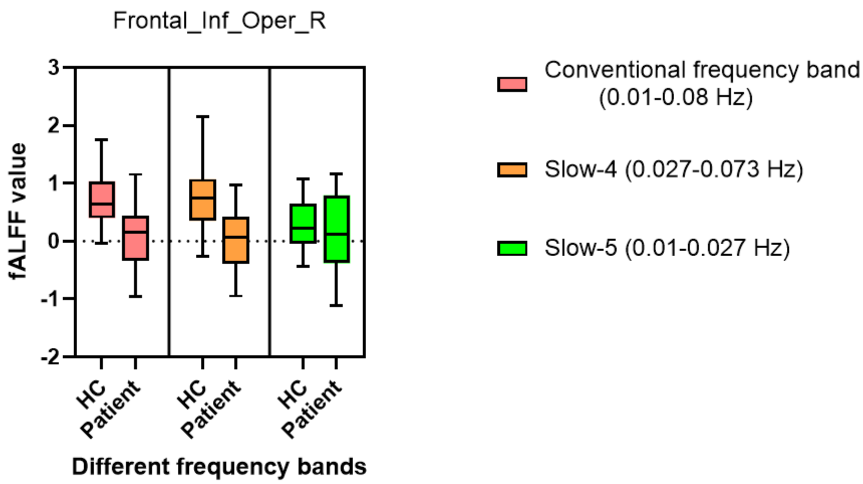

Figure S54 The fALFF value of Frontal_Inf_Oper_R in different frequency bands. fALFF, fractional amplitude of low-frequency fluctuation.

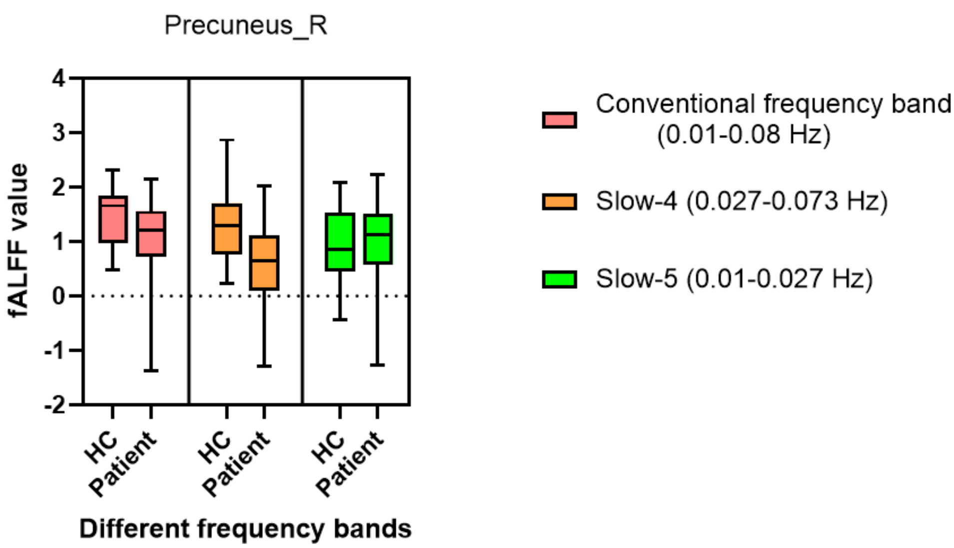

Figure S55 The fALFF value of Precuneus_R in different frequency bands. fALFF, fractional amplitude of low-frequency fluctuation.

 https://dx.doi.org/10.21037/qims-22-17

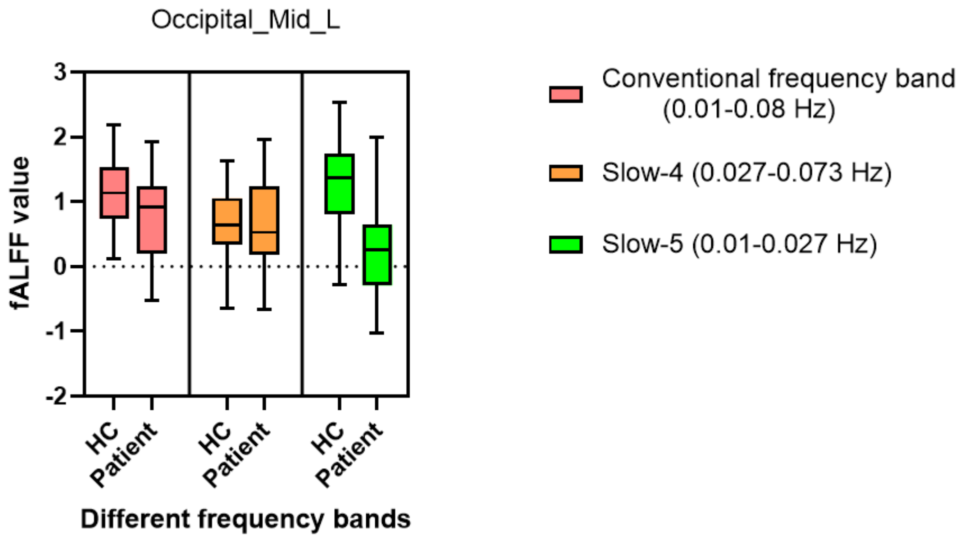

Figure S56 The fALFF value of Occipital_Mid_L in different frequency bands. fALFF, fractional amplitude of low-frequency fluctuation.

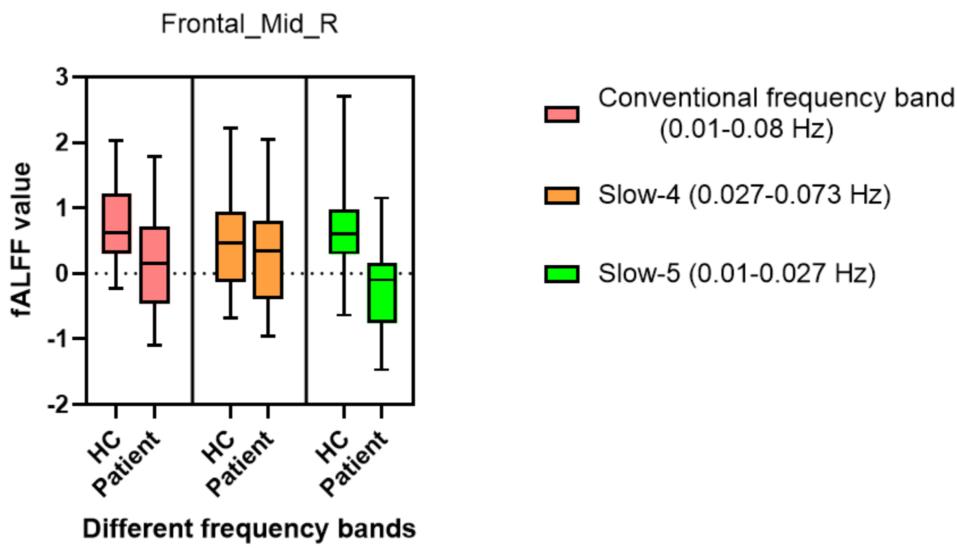

Figure S57 The fALFF value of Frontal_Mid_R in different frequency bands. fALFF, fractional amplitude of low-frequency fluctuation.

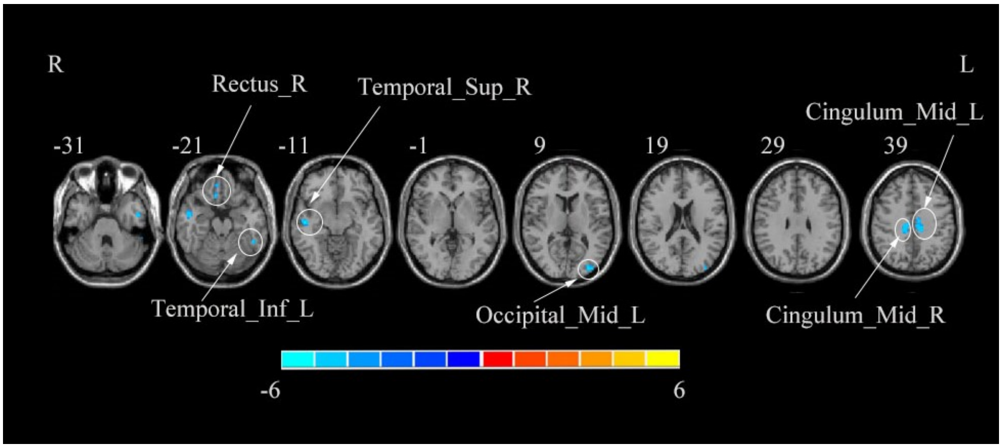

Figure S58 Results of the VBM comparisons between patients with intracranial tuberculosis and healthy controls.

Table S1 Results of partial correlation analysis between aberrant ALFF and neuropsychological performances

	MMSE		DST_forwards	
	r	P	r	P
HC				
Slow-5				
Supp_Motor_Area_L	0.538	0.004*	-	-
Patient				
Conventional frequency band				
Paracentral_Lobule_R	-	-	0.524	0.004*

*P<0.05. ALFF, amplitude of low-frequency fluctuation.

https://dx.doi.org/10.21037/qims-22-17

Table S2 Results of partial correlation analysis between aberrant fALFF and neuropsychological performances

	MMSE		RAVLT_I		RAVLT_II		RAVLT		DST_forwards		MoCA		CDT		SDMT	
	r	P	r	P	r	P	r	P	r	P	r	P	r	P	r	P
HC																
conventional frequency band																
Cerebelum_9_L	-	-	0.514	0.006*	0.447	0.019*	0.532	0.004*	-	-	-	-	-	-	0.413	0.032*
Parietal_Inf_L	0.426	0.027*	-	-	-	-	-	-	-	-	-	-	-	-	-	-
slow-4																
Precuneus_R	-	-	0.414	0.032*	-	-	-	-	-	-	-	-	-	-	-	-
slow-5																
Occipital_Mid_L	-	-	-	-	-	-	-	-	-	-	0.539	0.004*	-	-	-	-
Frontal_Mid_R	-	-	-	-	-	-	-	-	-	-	-	-	-0.501	0.008*	-	-
Patient																
Conventional frequency band																
Frontal_Inf_ Oper_R	-0.451	0.016*	-	-	-	-	-	-	-	-	-	-	-	-	-	-
Slow-4																
Precuneus_R	-	-	-	-	-	-	-	-	-0.389	0.041*	-	-	-	-	-	-

fALFF, fractional amplitude of low-frequency fluctuation.

Table S3 Results of the VBM comparisons between patients with intracranial tuberculosis and healthy controls

Regions (AAL)	BA	Peak MNI Coordinates (mm)			Cluster Size	Peak T-value
		X	Y	Z		
Temporal_Inf_L	20	-49.5	-3	-33	249	-5.3566
Temporal_Inf_L	37	-48	-46.5	-21	201	-4.4957
Rectus_R	11	9	31.5	-24	251	-4.7916
Temporal_Sup_R	21	52.5	-13.5	-10.5	372	-5.047
Occipital_Mid_L	19	-33	-88.5	10.5	452	-5.0248
Cingulum_Mid_L	24	-6	-22.5	43.5	563	-4.9851
Cingulum_Mid_R	31	12	-21	40.5	411	-4.8805

Specific steps for VBM analysis as follows: All the structural images were processed and examined using the CAT12 toolbox (http:// dbm.neuro.uni-jena.de/cat/) implemented in SPM12 (http:// www.fil.ion.ucl.ac. uk/spm/software/spm12/) for VBM analysis running in MATLAB2017b. All images were segmented into grey matter (GM), white matter (WM), and cerebrospinal fluid (GSF), and then underwent a quality control to check sample homogeneity. NO images had to be excluded due to poor quality. All GM scans were smoothed with a Gaussian kernel of 6 mm (FWHM). We applied an absolute masking threshold of 0.1 to the VBM data. After the smooth, GM images were performed two-sample t-tests in RESTplus. TIV as covariates. False discovery rate (FDR) correction was performed and P<0.05 was considered significant.